(ค)

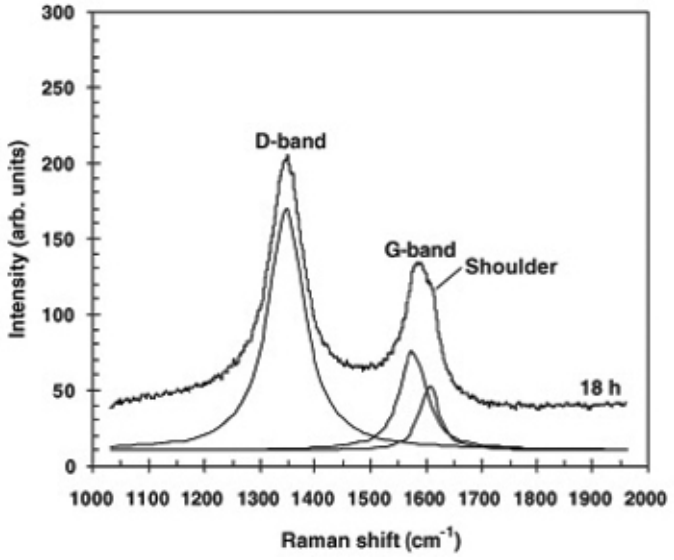

(ง)

รูปที่ 27. Raman spectra ของ MWNTs (as-grown) ที่สังเคราะห์ในเวลา (ก-ง) 1, 6, 12 และ 18 h ตามลำดับ

ตารางที่ 3. Raman shift และ intensity ratios ที่ได้จาก Raman spectra

Synthesized time (h)	D-band (cm^{-1})	G-band (cm^{-1})	Shoulder (cm^{-1})	I_D/I_G	I_S/I_G
1	1,349	1,575	1,604	0.84	0.21
6	1,351	1,578	1,606	0.90	0.21
12	1,349	1,573	1,604	1.17	0.22
18	1,348	1,577	1,606	2.37	0.27

Electrical property

I-V curves ของ MWNTs เปรียบเทียบกับของ graphite powder ได้แสดงไว้ในรูปที่ 28 ซึ่งมีลักษณะเป็นแบบเส้นตรง โดย resistivity ที่ต่ำที่สุดสำหรับ 1 h มีค่าประมาณ 0.53 ohm.cm สำหรับ graphite powder มีค่าเป็น 1.06 ohm.cm และสำหรับ hot pressed sintered CNTs มีค่าเป็น 10^{-4} ohm.cm [26] ทั้งนี้น่าจะเกิดจาก inter-tubes contact ที่ต่างกัน [27]

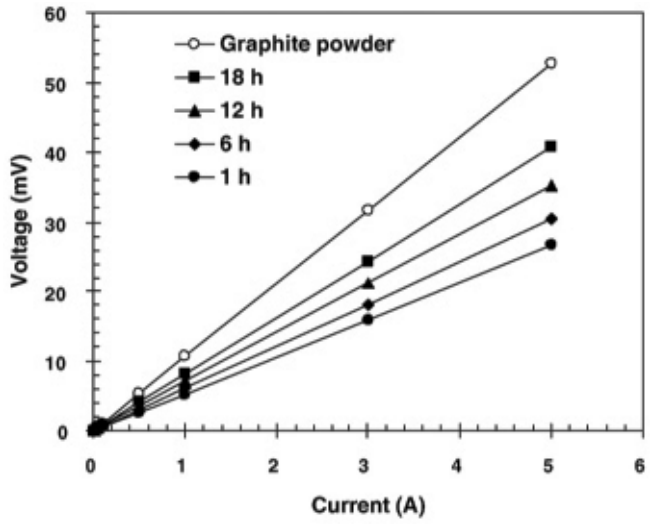

รูปที่ 28. I-V curves ของ MWNTs (as-grown) และ graphite powder

Intensity ratio **และ** electrical resistivity

รูปที่ 29 เปรียบเทียบกันระหว่าง I_D/I_G และ resistivity ของ MWNTs (as-grown) ซึ่งแสดงถึงการเพิ่มขึ้นของ I_D/I_G และ resistivity ตามเวลาการสังเคราะห์ที่เพิ่มขึ้น แสดงว่ามี defect เกิดมากขึ้นด้วย ซึ่งน่าจะเกิดจากการมี OH radical ที่เกิดมากขึ้นและจะไปทำลาย ordering ของ carbon atoms ใน MWNTs [28,29]

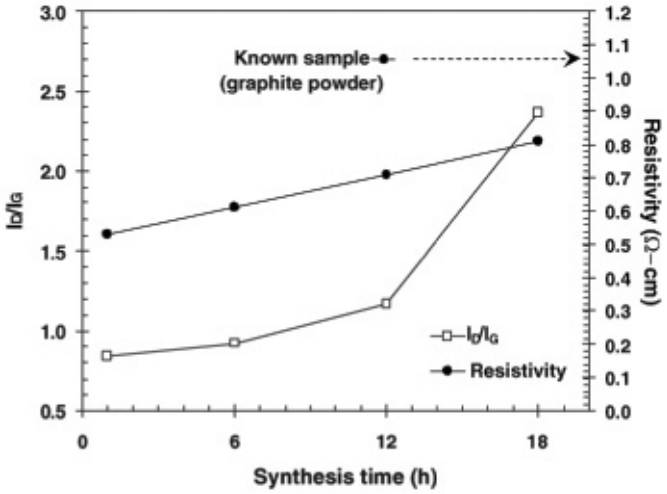

รูปที่ 29. I_D/I_G และ resistivity ของ MWNTs (as-grown) ที่เวลาการสังเคราะห์ต่าง ๆ

สรุปผลการทดลอง

อาจทำการสังเคราะห์ Fe-deposited dots บน substrates ที่เป็น stainless steel และ glass slide โดยการ spark ด้วยลวด Fe ที่ applied voltages ต่าง ๆ จาก surface analysis พบว่า RMS values, mean roughness และ maximum height มีค่าเพิ่มขึ้นตามจำนวนครั้งในการ spark ที่เพิ่มขึ้น นอกจากนี้ยังพบว่า RMS values และ height ของ dots มีความอ่อนไหวต่อ applied voltages ในการทดลองนี้ไม่สามารถสังเคราะห์ CNTs บน stainless steel และ glass substrates โดยไม่ใช้ catalyst ได้ การเติบโตของ CNTs บน Fe-deposited dots ซึ่งมีลักษณะคล้ายส่วนหนึ่งของ sphere เกิดขึ้นได้ทุกทิศทาง โดย CNTs ที่สังเคราะห์ได้นี้มีทั้งชนิดตรงและโค้งงอ โดย growth rate มีค่า

เอกสารอ้างอิง

[1] Y. Shingaya, T. Nakayama, M. Aono, Phys. B, 323 (2002) 153

[2] Y. Saito, K. Hata, A. Takakura, J. Yotani, S. Uemura, Phys. B, 323 (2002) 30

[3] Y. Homma, T. Yamashita, Y. Kobayashi, T. Ogino, Phys. B, 323 (2002) 122

[4] J. Wei, H. Zhu, D. Wu, B. Wei, Appl. Phys. Lett., 84 (2004) 4869

[5] K. Tsukagoshi, N. Yoneya, S. Uryu, Y. Aoyagi, A. Kanda, Y. Ootuka, B.W. Alphenaar, Phys. B, 323 (2002) 107

[6] D. Sarangi, I. Arfaoui, J.M. Bonard, Phys. B, 323 (2002) 165

[7] D. Pradhan, M. Sharon, Mater. Sci. & Eng. B, 96 (2002) 24

[8] Z. Wang, Z. Liang, B. Wang, C. Zhang, L. Kramer, Composites A, 35 (2004) 1225

[9] J.I. Sohn, C. Nam, S. Lee, Appl. Surf. Sci., 197-198 (2002) 568

[10] C.J. Lee, J. Park, J.A. Yu, Chem. Phys. Lett, 360 (2002) 250

[11] C.L. Lin, C.F. Chen, S.C. Shi, Diam. & Relat. Mater., 13 (2004) 1026

[12] I. Mukhopadhyay, S. Kawasaki, F. Okino, A. Govindaraj, C.N.R. Rao, H. Touhara, Phys. B, 323 (2002) 130

[13] J.C. Bae, Y.J. Yoon, S.J. Lee, H.K. Baik, Phys. B, 323 (2002) 168

[14] A.C. Dillon, P.A. Parilla, J.L. Alleman, J.D. Perkins, M.J. Heben, Chem. Phys. Lett, 316 (2000) 13

[15] J.M.C. Moreno, S.S. Swamy, T. Fujino, M. Yoshimura, Chem. Phys. Lett, 329 (2000) 317

[16] G.S. Duesberg, R. Graupner, P. Downes, A. Minett, L. Ley, S. Roth, N. Nicoloso, Synth. Met., 142 (2004) 263

[17] Powder Diffract. File, JCPDS Internat. Centre for Diffract. Data, PA 19073-3273, U.S.A., (2001)

[18] C.J. Lee, S.C. Lyu, H.W. Kim, J.W. Park, H.M. Jung, J. Park, Chem. Phys. Lett., 361 (2002) 469

[19] S. Honda, Y.G. Baek, K.Y. Lee, T. Ikuno, T. Kuzuoka, J.T. Ryu, S. Ohkura, M. Katayama, K. Aoki, T. Hirao, K. Oura, Thin Solid Films, 464-465 (2004) 290

[20] G.N. Fursey, D.V. Novikov, G.A. Dyuzhev, A.V. Kotcheryzhenkov, P.O. Vassiliev, Appl. Surf. Sci., 215 (2003) 135

[21] Y.M. Wong, S. Wei, W.P. Kang, J.L. Davidson, W. Hofmeister, J.H. Huang, Y. Cui, Diam. Relat. Mater., 13 (2004) 2105

[22] O.A. Nerushev, M. Sveningsson, L.K.L. Falk, F. Rohmund, J. Mater. Chem., 11 (2001) 1122

[23] Y. Chen, S.Z. Deng, N.S. Xu, J. Chen, X.C. Ma, E.G. Wang, Mater. Sci. Eng. A, 327 (2002) 16

[24] K.W. Andrews, D.J. Dyson and S.R. Keown, Interpret. Electr. Diffract. Patter., 2nd ed, Plenum Press, NY, (1971)

[25] A.M. Valiente, P.N. López, I.R. Ramos, A.G. Ruiz, C. Li, Q. Xin, Carbon, 38 (2000) 2003

[26] R.Z. Ma, C.L. Xu, B.Q. Wei, J. Liang, D.H. Wu, D.J. Li, Mater. Res. Bull., 34 (1999) 741

[27] A.G. Rinzler, J. Liu, H. Dai, P. Nikolaev, C.B. Huffman, F.J. Rodríguez-Macías, P.J. Boul, A.H. Lu, D. Heymann, D.T. Colbert, R.S. Lee, J.E. Fischer, A.M. Rao, P.C. Eklund, R.E. Smalley, Appl. Phys. A, 67 (1998) 29

[28] S. Maruyama, R. Kojima, Y. Miyauchi, S. Chiashi, M. Kohno, Chem. Phys. Lett., 360 (2002) 229

[29] K. Hata, D.N. Futaba, K. Mizuno, T. Namai, M. Yumura, S. Iijima, Sci., 306 (2004) 1362

Output ที่ได้จากโครงการ

1. สามารถเผยแพร่ผลงานวิจัยได้จำนวน 5 เรื่อง และผลิตบัณฑิตศึกษาได้จำนวน 5 ท่าน
2. ได้รับเชิญให้เป็น distinguished speaker ในการประชุม "2nd International Symposium on Creation of Hybridized Materials with Super-Functions and Formation of International Research & Education Center" Nagaoka, Japan, 19-21 Jan 2004 และ ในการประชุม 8th International Symposium on Eco-Materials Processing and Design (ISEPD 2007) 11-14 January 2007, Kitakyushu, Japan
3. เป็น International Advisory Committee ใน Materials Science Forum, Vol 510-511, 2006 และ ใน Materials Science Forum, Vol 544-545, 2007
4. เป็น International Advisory Committee ในการประชุม 7th International Symposium on Eco-Materials Processing and Design (ISEPD 2006) 8-11 January 2006, Chengdu, China และ ในการประชุม 8th International Symposium on Eco-Materials Processing and Design (ISEPD 2007) 11-14 January 2007, Kitakyushu, Japan
5. ได้รับการแต่งตั้งให้เป็นกรรมการวิชาการสาขาฟิสิกส์ เพื่อตรวจสอบบทคัดย่อสาขาวิชาฟิสิกส์ที่จะนำเสนอในการประชุม วทท 32 (ตุลาคม 2549)
6. เป็น reviewer เพื่อตรวจสอบ manuscript ที่จะตีพิมพ์ใน Journal of Materials Science, Surface and Coatings Technology, Materials Science and Engineering A, Solid State Phenomena, วารสารวิจัยและพัฒนา มหาวิทยาลัยเทคโนโลยีพระจอมเกล้าธนบุรี และ Chiang Mai Journal of Science

ภาคผนวก

Materials Science Forum Vols. 510-511 (2006) pp. 470-473
online at http://www.scientific.net

Growth of CNTs on 304 Stainless Steel Using Sparked Iron as a Catalyst

Somchai Thongtem*, Pisith Singjai, Titipun Thongtem and Suphaporn Daothong
Faculty of Science, Chiang Mai University, Chiang Mai 50200, Thailand
E-mails : schthongtem@yahoo.com and sthongtem@hotmail.com
* Corresponding Author

Keywords : Carbon nanotubes, Sparked iron dots, Stainless steel substrates

Abstract. Carbon nanotubes (CNTs) were grown on 304 stainless steel using iron as a catalyst. By using the applied voltages of 4-6 kV, iron wire with 0.5 mm in diameter was sparked for 1, 2, 10 and 100 times to form catalytic dots on the steel substrate. CNTs were subsequently grown in a gas mixture of 10 ml/s Ar and 0.1 ml/s C_2H_2 at a temperature range 700 - 900 K for 300 s (5 min). The dots and CNTs were characterised using AFM, SEM and TEM to determine their characteristics.

1. Introduction

Due to the small dimension and remarkable properties of carbon nanotubes (CNTs), they have been considered for use in a variety of applications. Among them are flat panel displays [1], nanoelectronics [2], household light bulbs [3], interconnection of nanostructures [4], nanotips [5], electrode support materials [6], and others. CNTs can be grown by several methods; for example, chemical vapor deposition (CVD) [7-9], graphite arc-discharge [10], electrophoresis [11], laser annealing [12], and hydrothermal [13]. The CVD is regarded as one of the most promising method used for the CNT growing. For simplicity, a single gas is used in most of the researches but multiple gas phases are used in industrial processes. The reactive gas used as carbon source is selected on the basis of the catalytic metals [14]. For the present research, an iron wire was sparked to form catalytic dots/islands on stainless steel substrate. By using the CVD method, CNTs were grown in flowing Ar containing C_2H_2 at high temperature in a homemade reaction chamber. The characteristics of the dots and CNTs were then studied.

2. Experiment

Stainless steel type 304 used as a substrate was polished down with 0.1 micron alumina powder and degreased with alcohol prior to the test. By using 4-6 kV, Fe wire with 0.5 mm in diameter was sparked to form Fe dots/islands. The Fe-deposited substrate was hung in a high-alumina porcelain reaction chamber which was fired at 1,573 K. The substrate was heated in 10 ml/s Ar until the test temperature was obtained at 700-900 K and 0.1 ml/s C_2H_2 was added for 300 s (5 min). At the conclusion of the process, the substrate was left to cool down in the flowing Ar to room temperature and further analysed using an atomic force microscope (AFM), a scanning electron microscope (SEM) and a transmission electron microscope (TEM).

3. Results and Discussion

3.1 Fe-deposited Dots

By using 6 kV, Fe wire with 0.5 mm in diameter was sparked to form Fe-deposited dots on stainless steel substrates. Then, they were analyzed using AFM and the results are shown in Fig 1. A number of Fe-deposited dots was detected. The deposition did not form a regular pattern. Over the 1 μm x 1 μm on stainless steel substrates, root mean square (RMS) values, mean roughness and maximum height for a variety of sparking number are summarised in Table 1. These show that they are increased with an increase of the sparking number. Sometimes the dots may slide on the

substrate due to the sparking force as shown in Fig 2. The latter dots may collide with the former dots and they are fastened together. These can lead to the irregular dots on the substrates.

By using 4, 5 and 6 kV, the stainless steel substrates were sparked for 10 times. Section analysis over a distance of 1 μm is shown in Fig 3. The irregular patterns were detected. The RMS values at 4, 5 and 6 kV are 11.038, 12.169 and 13.687 nm, respectively. This shows that they are sensitive to the applied voltages. The height of the dots is increased with an increase of the applied voltages as well as of the sparking number.

Table 1. RMS values, mean roughness and maximum height over 1 μm x 1 μm in area for a variety of the sparking number.

Sparking number	RMS values(nm)	Mean roughness(nm)	Maximum height(nm)
1	3.695	2.639	36.330
2	3.714	2.687	47.313
10	14.572	11.530	120.23
100	30.987	24.616	222.33

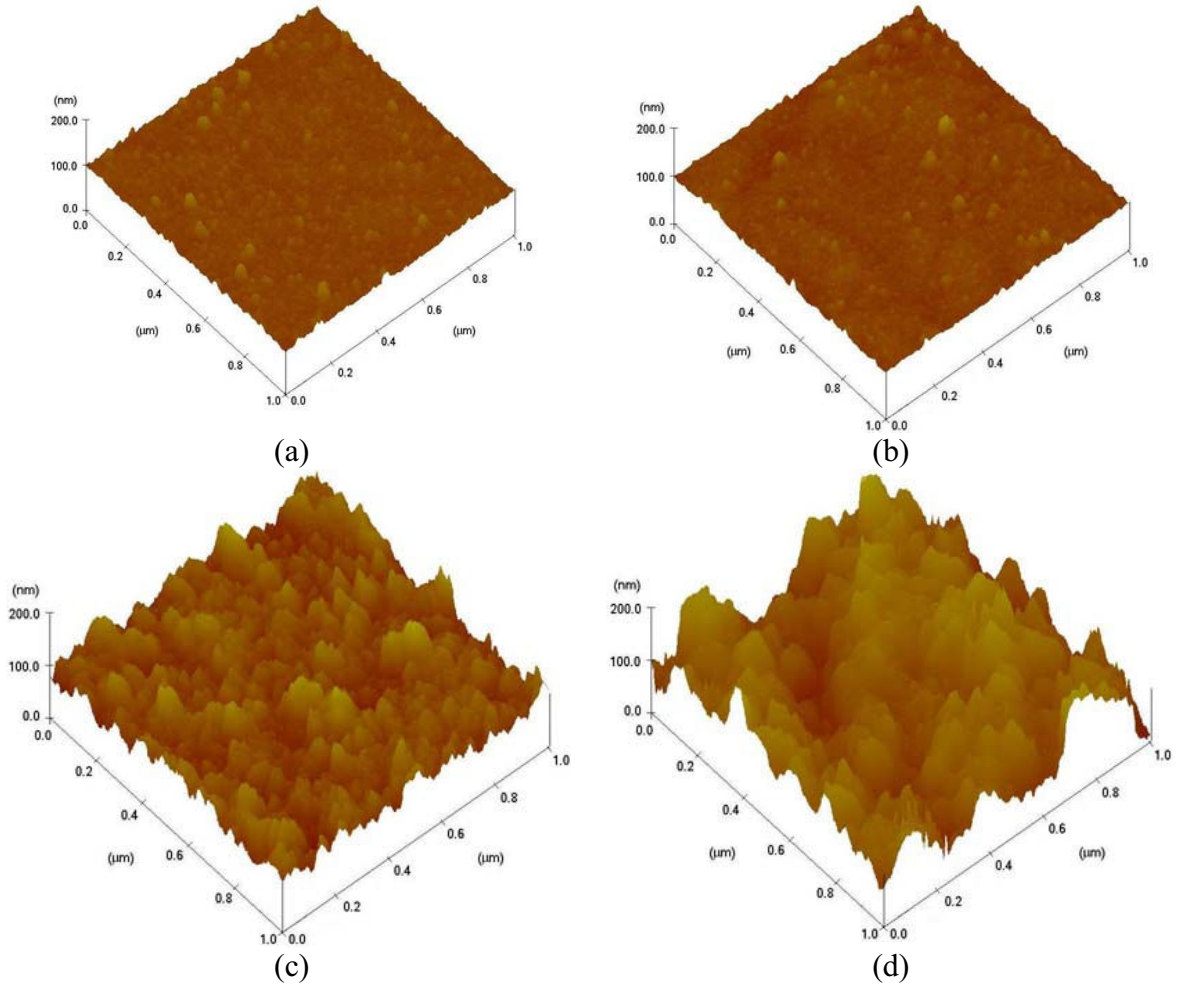

Fig 1. AFM analysis of Fe-deposited dots on 1 μm x 1 μm stainless steel substrates using 6 kV. (a)-(d) Sparking for 1, 2, 10 and 100 times, respectively.

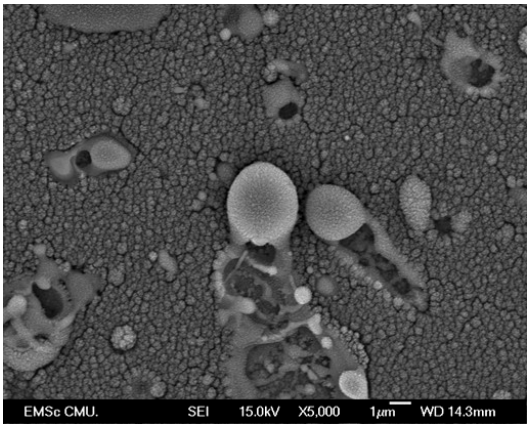

Fig 2. SEM micrograph of Fe deposited dots on the substrate using 6 kV for 100 sparking.

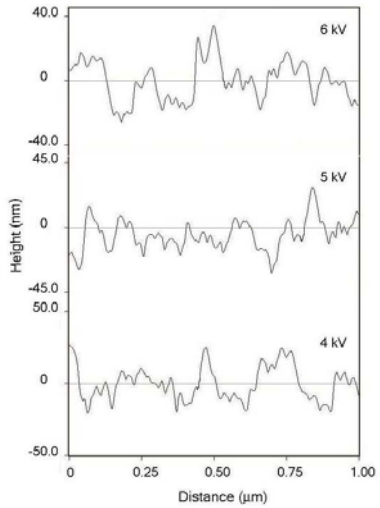

Fig 3. Section analysis of the substrates sparked for 10 times by using the applied voltages of 4, 5 and 6 kV.

3.2 Growth of CNTs

The stainless steel substrate without Fe depositing on top was used for CNT growing at 900 K but no CNTs were detected. This shows that CNTs can not be grown on the substrate without any catalysts. For the present research, Fe was sparked on the steel substrates to form catalytic dots. CNTs were subsequently grown at high temperature and SEM micrographs are shown in Fig 4. The CNTs can grow in all directions with a variety of shapes and sizes. Some CNTs can be grown although the temperature is as low as 700 K. The number of sparking may not play a role on the CNT growing. Comparing between the growth at 700 K and 900 K, the CNTs grown at 900 K are longer than those at 700 K. The maximum growth rates at 700 and 900 K are 6.2 and 16 nm/s, respectively. Growth rate is very sensitive to the temperature. At each temperature, some CNTs are short and some are long showing that their initiation is very different from each other.

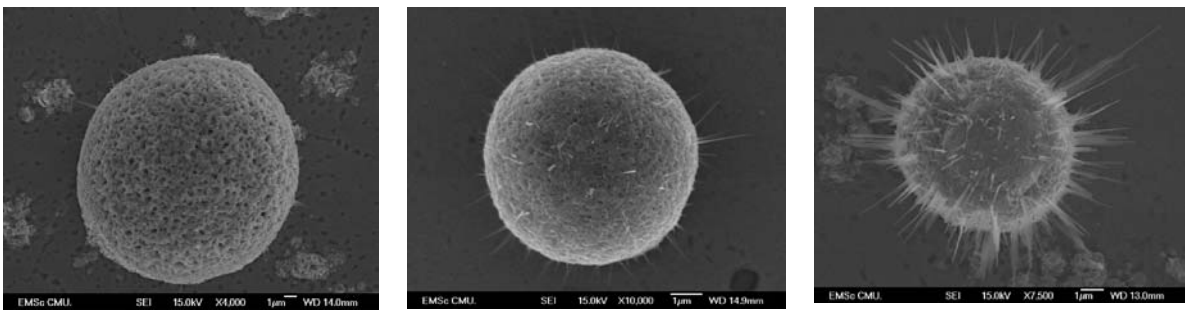

(a) (b) (c)

Fig 4. SEM micrographs of CNTs for a variety of sparking numbers and temperatures. (a) 1 time / 700 K, (b) 10 times / 700 K and (c) 10 times / 900 K.

3.3 CNT Characteristics

The CNTs grown at 900 K were put in a beaker containing deionised water and ultrasonically vibrated. The CNT-dispersed water was dropped on a copper grid, dried in ambient atmosphere and analysed using TEM. The TEM image and electron diffraction (ED) pattern are shown in Fig 5. The CNT is irregular surface showing that it is not perfect. It contains some defects and disordering atoms. Thickness of the CNT is about 16 nm. The ED pattern shows four concentric rings corresponding to (002), (101), (004) and (112) planes. The maximum intensity is the ring that diffracts from (002) plane. Comparing to the JCPDS [15], the diffraction pattern corresponds to carbon with hexagonal structure. The diffraction rings are not clearly sharp showing that the CNT contains some disordering atoms.

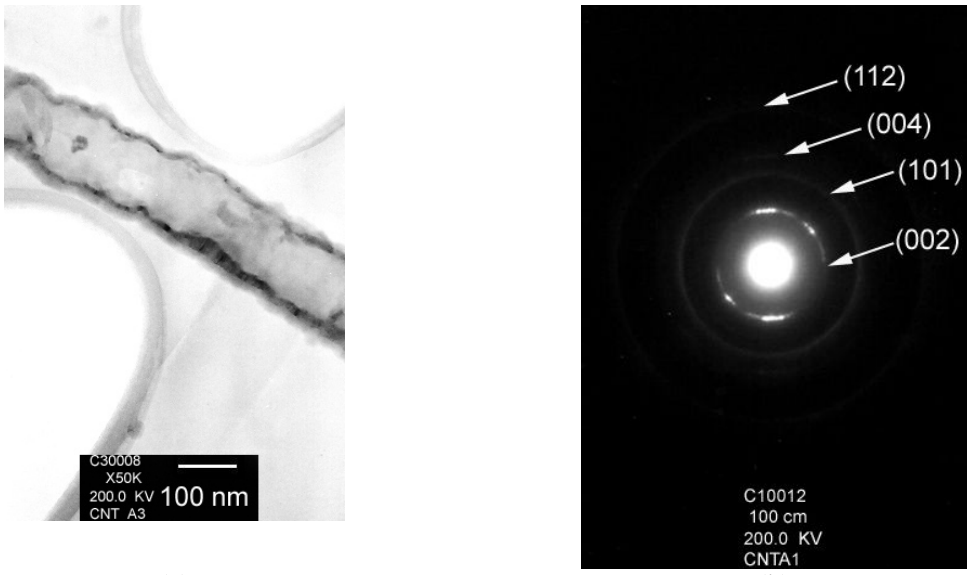

(a) (b)

Fig 5. (a) TEM and (b) ED pattern of CNT grown at 900 K.

4. Conclusions

Fe-deposited dots can be formed on stainless steel substrates by sparking of iron wire. Surface analysis shows that RMS values, mean roughness and maximum height are increased with an increase of the sparking number. In addition, RMS values and the height of the dots revealed by section analysis were found to be very sensitive to the applied voltages. No CNTs can be grown on the steel substrate without any catalyst. After sparking of Fe on the substrates, the CNTs can be grown in all directions at 700-900 K. Growth rate is increased with an increase of the temperature. The maximum growth rate at 900 K is 16 nm/s. For the present research, carbon with hexagonal structure was detected.

Acknowledgement

We are grateful to The Thailand Research Fund, Bangkok, for funding the research.

References

1. D. Sarangi, I. Arfaoui and J.M. Bonard, Phys. B323, 165(2002).
2. K. Tsukagoshi, N. Yoneya, S. Uryu, Y. Aoyagi, A. Kanda, Y. Ootuka and B.W. Alphenaar, Phys. B323, 107(2002).
3. J. Wei, H. Zhu, D. Wu and B. Wei, Appl. Phys. Lett. 84, 4869(2004).
4. Y. Homma, T. Yamashita, Y. Kobayashi and T. Ogino, Phys. B323, 122(2002).
5. Y. Shingaya, T. Nakayama and M. Aono, Phys. B323, 153(2002).
6. R.L.V. Wal and L.J. Hall, Carbon 41, 659(2003).
7. C. Liu, Y.C. Chen and Y. Tzeng, Diam. Relat. Mater. 13, 1274(2004).
8. S. Honda, Y.G. Baek, K.Y. Lee, T. Ikuno, T. Kuzuoka, J.T. Ryu, S. Ohkura, M. Katayama, K. Aoki, T. Hirao and K. Oura, Thin Solid Film. 464-465, 290(2004).
9. E. Flahaut, Ch. Laurent and A. Peigney, Carbon 43, 375(2005).
10. I. Mukhopadhyay, S. Kawasaki, F. Okino, A. Govindaraj, C.N.R. Rao and H. Touhara, Phys. B323, 130(2002).
11. J.C. Bae, Y.J. Yoon, S.J. Lee and H.K. Baik, Phys. B323, 168(2002).
12. S. Botti, R. Ciardi, L. Asilyan, L.D. Dominicis, F. Fabbri, S. Orlanducci and A. Fiori, Chem. Phys. Lett. 400, 264(2004).
13. Y. Gogotsi, J.A. Libera and M. Yoshimura, J. Mater. Res. 15, 2591(2000).
14. P.N. López, I.R. Ramos and A.G. Ruiz, Carbon 41, 2509(2003).
15. Powder Diffract. File, JCPDS Internat. Centre for Diffract. Data, PA 19073-3273, U.S.A., (2001).

ELSEVIER

Materials Science and Engineering A 423 (2006) 209–213

MATERIALS SCIENCE & ENGINEERING A

www.elsevier.com/locate/msea

Growth of carbon nanoflowers on glass slides using sparked iron as a catalyst

Somchai Thongtem *, Pisith Singjai, Titipun Thongtem, Suksawat Preyachoti

Faculty of Science, Chiang Mai University, Chiang Mai 50200, Thailand

Received 8 July 2005; received in revised form 15 September 2005; accepted 30 September 2005

Abstract

Carbon nanotubes (CNTs) were grown on glass slides using iron as a catalyst. By using 6 kV voltage, iron wire with 0.5 mm in diameter was sparked for 1, 2, 10 and 100 times to form iron dots/islands on the slides. CNTs were subsequently grown in a gas mixture of 10 ml/s Ar and 0.1 ml/s C_2H_2 at a temperature range of 700–900 K for 300 s (5 min). In scanning and transmission electron microscopies, the CNTs grown on iron dots appear like flowers composed of carbon with hexagonal structure. In addition, the effects of oxide and gold sputtering on the growth of CNTs were studied. Both have no major influence on the growth.

Keywords: Carbon nanotubes; Sparked iron; Glass slides

1. Introduction

Since the discovery of carbon nanotubes (CNTs), they have been intensively studied by a number of researchers. The CNTs show very interesting properties and can be used as nanotip for scanning tunnelling microscopy (STM) [1], electron sources of ultra-high luminance light-source devices [2], interconnection of nanostructures [3], household light bulbs [4], nanoelectronics [5], flat panel displays [6], nanofilaments and nanobeads [7], single-walled carbon nanotube (SWNT) buckypaper/epoxy resin matrix nanocomposites [8] and many others. They can be grown by several methods. Among them are chemical vapor deposition (CVD) [9–11], graphite arc-discharge [12], electrophoresis [13], laser pulse power [14] and hydrothermal [15,16]. The CVD is regarded as one of the most promising method used for the CNT growing. Fe, Co and Ni are known as the most effective catalysts used in this process [10]. Their functions are to promote the decomposition of carbon precursors, diffusion of carbon atoms, formation of metastable carbides and graphitic sheets and others [10]. For the present research, an iron wire was sparked to form catalytic dots/islands on glass slides. By using the CVD method, CNTs were grown in flowing Ar containing C_2H_2 at high temperature. Then, the effects of the catalyst, temperature, oxide formation and Au sputtering on the CNT growing were studied.

2. Experiment

A glass slide was used as a substrate and its composition analysed by energy-dispersive X-ray spectrometry (EDX) is shown in Table 1. The slide was degreased with alcohol prior to the test. By using 6 kV, Fe wire with 0.5 mm in diameter was sparked to form Fe dots/islands. The Fe-deposited slide was hung in a high temperature reaction chamber into which Ar was fed for removal of air. The slide was heated in 10 ml/s Ar until the test temperature was obtained at 700–900 K and 0.1 ml/s C_2H_2 was added for 300 s (5 min). The growth of CNTs was done at 1 atm pressure. At the conclusion of the process, the slide was left to cool down in the flowing Ar to room temperature and further analysed using a scanning electron microscope equipped with EDX and a transmission electron microscope operated at 15.0 and 200.0 kV, respectively.

3. Results and discussion

3.1. Effect of catalyst

The slide used for the study composes of Na, Mg, Al, Si, Ca and O showing that it composes of oxides of the metals. The

* Corresponding author. Tel.: +66 53 240 989; fax: +66 53 892 271.
E-mail addresses: schthongtem@yahoo.com, sthongtem@hotmail.com (S. Thongtem).

0921-5093/$ – see front matter © 2006 Elsevier B.V. All rights reserved.
doi:10.1016/j.msea.2005.09.125

Table 1
EDX analysis (K line) of the glass slide

Element	wt.%	at.%
O K	47.68	61.17
Na K	8.72	7.78
Mg K	2.70	2.28
Al K	0.29	0.22
Si K	35.42	25.89
Ca K	5.19	2.66
Total	100.00	100.00

slide was used as a substrate for growing of CNTs at 900 K but no CNTs were detected. This shows that CNTs cannot be grown on the slide without any catalysts. Therefore, Fe was deposited on glass slides by sparking for 1, 2, 10 and 100 times to form catalytic dots. After sparking for 100 times, the dots dispersed in all directions. Their sizes are decreased with the increasing of distance. The number of the dots are increased with an increasing of the sparking number. However, the former can be collided by the latter and they are fastened together. Then, CNTs were subsequently grown at 900 K and the selected scanning electron microscopy (SEM) images are shown in Fig. 1. It was found that the sparking number did not play a role on the CNT growing. The Fe-deposited dots are similar to part of a sphere. Therefore, the CNTs were grown in all directions and are similar to flowers. They compose of a variety of shapes and sizes. The CNTs on the large dots are longer than those on the small dots. This shows that CNTs grow from the large dots before from the small dots and that CNTs grow on the large dots faster than they grow on the small dots. For the present condition, no CNTs can be grown on 1 μm dot (Fig. 1a). This shows that CNTs are likely to grow on the dots that are larger than 1 μm. In addition, no CNTs can be grown on the 50 nm Fe-deposited dots sparked for 100 times (Fig. 1d) either. The experimental time might be too short to obtain the long CNTs that can be detected by the SEM.

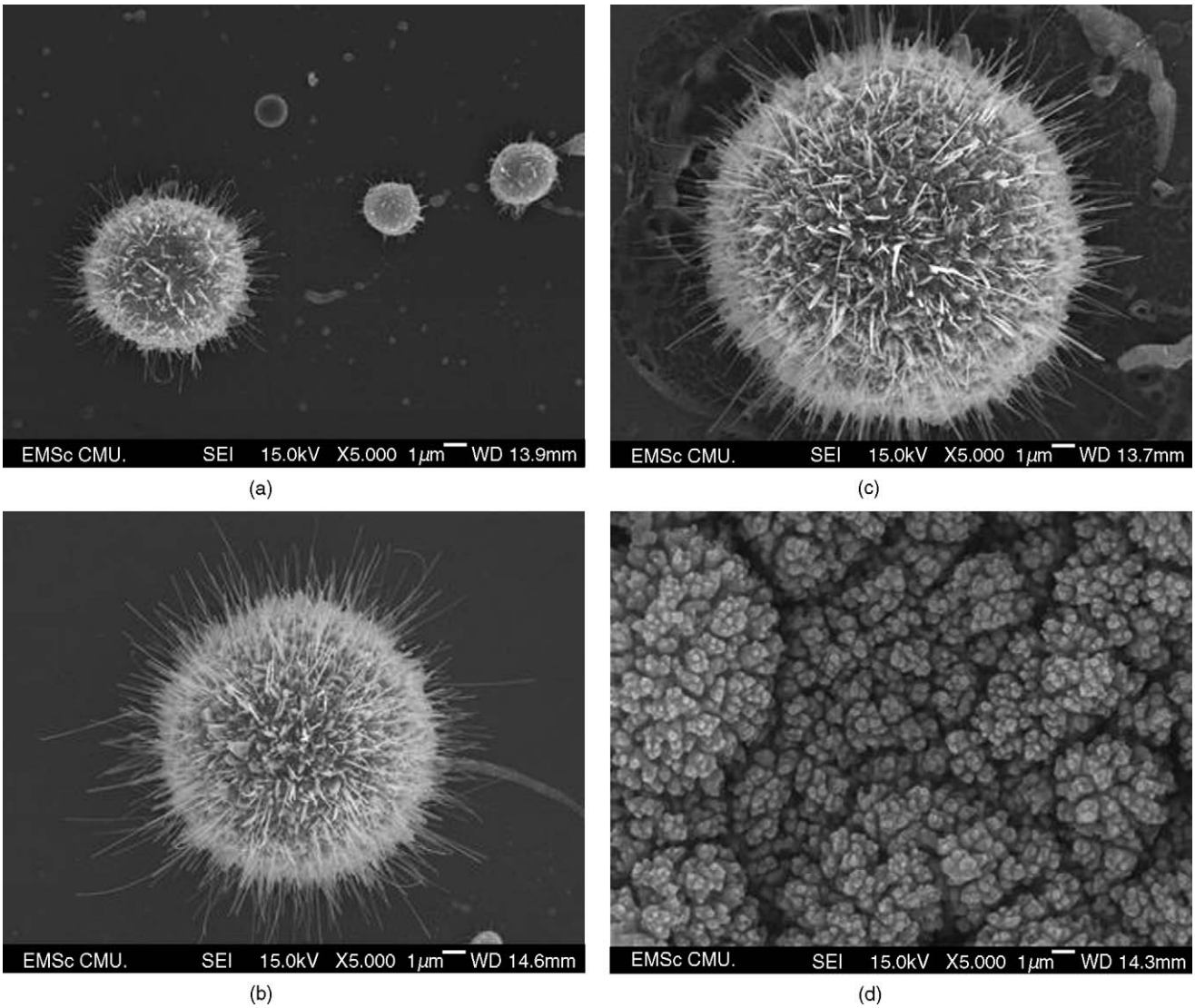

Fig. 1. Fe-deposited dots with CNT growing at 900 K (SEM images). Sparking for (a) 1, (b) 2, (c) 10 and (d) 100 times.

3.2. Effect of temperature

To determine the minimum temperature which CNTs can be grown, the glass sparked for 100 times was used for CNT growing at 700, 750, 800, 850 and 900 K. The results are shown in Fig. 2. At 700 K, a few of CNTs started to grow on Fe-deposited dots; especially, for those that are equivalent to or larger than 1 μm in diameter. At 750 K, some CNTs were clearly grown but

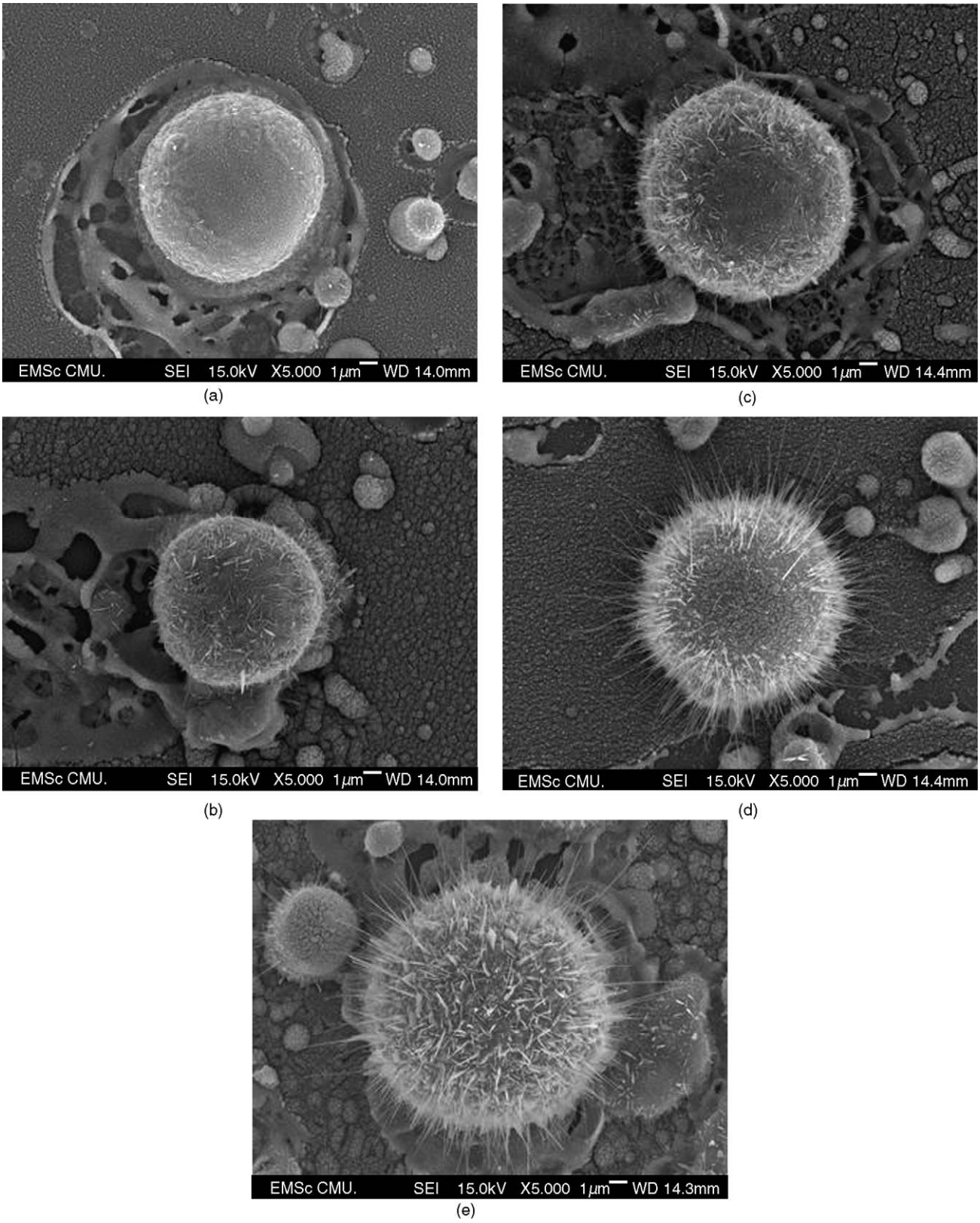

Fig. 2. SEM images of the CNTs grown on Fe-deposited dots at (a) 700, (b) 750, (c) 800, (d) 850 and (e) 900 K.

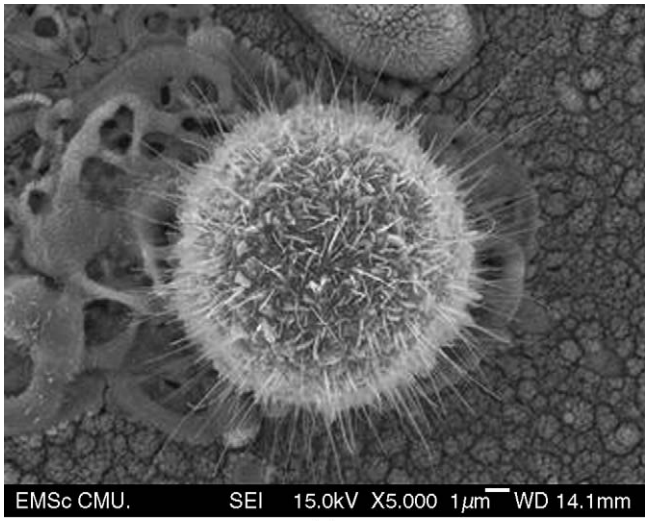

(a)

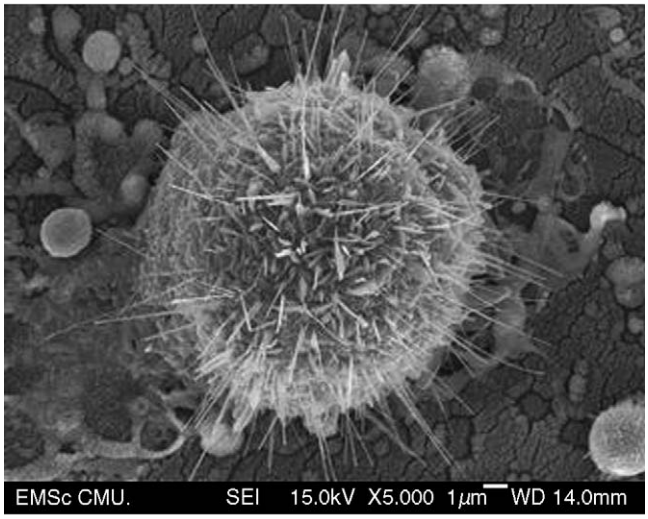

(b)

Fig. 3. The CNTs grown at 900 K on Fe-deposited dots (SEM images). (a) One week after sparking. (b) Sparking and leaving in alcohol for 24 h prior to the growth.

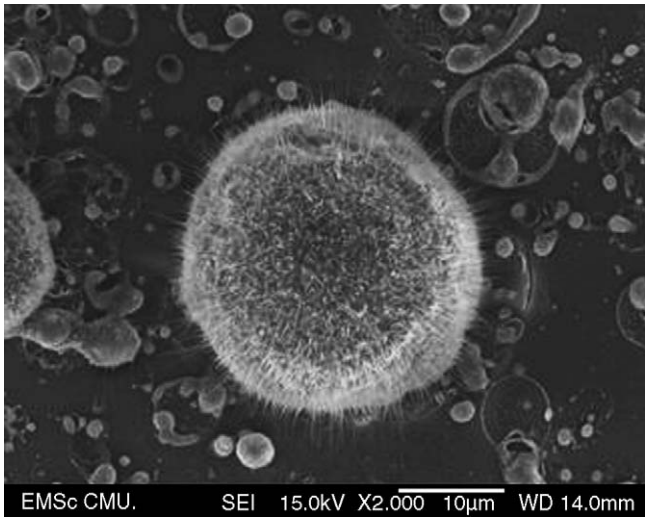

Fig. 4. SEM images of the CNTs grown on Au-sputtered slide.

they are quite short. The CNTs are longer at the higher temperature. For each temperature, some CNTs are short and some are long. Growth rate of the CNTs is increased with an increasing of the temperature. The maximum growth rate is at 900 K with the maximum value of 2.14×10^{-2} μm/s.

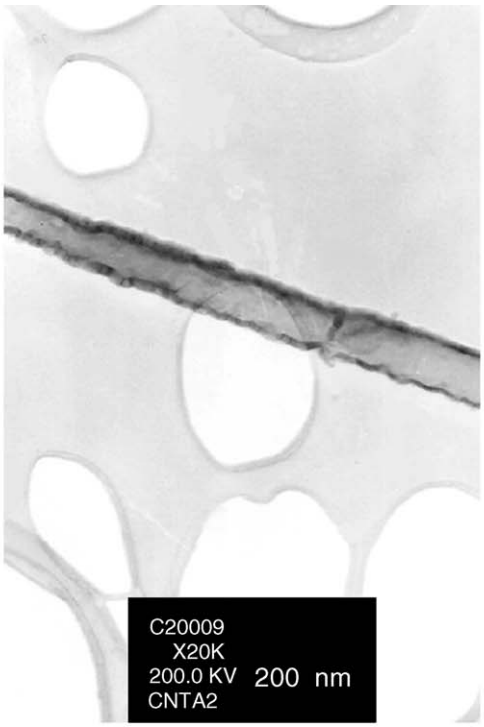

(a)

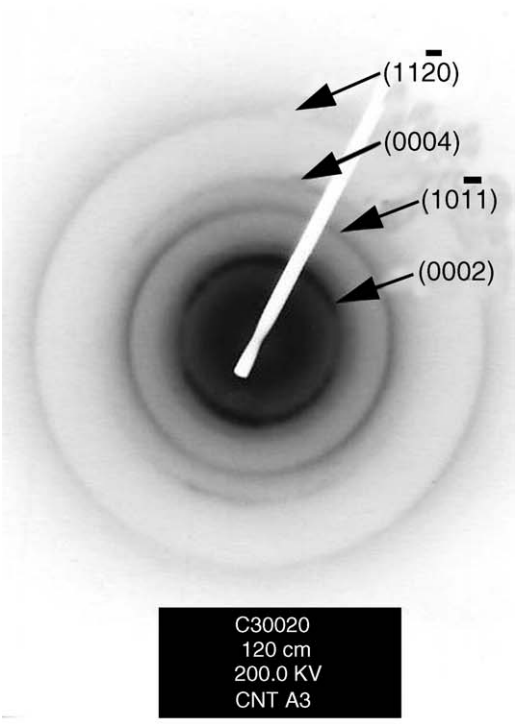

(b)

Fig. 5. (a) TEM image and (b) electron diffraction pattern of the CNT grown at 900 K.

3.3. Effect of oxide formation

Effect of oxide coated on Fe-deposited dots was studied. Instead of sparking and immediate growing the CNTs as above, glass slides were sparked for 100 times and left for oxide formation on the dots at a variety conditions before growing the CNTs at 900 K. The results are shown in Fig. 3. Comparing to the CNTs obtained by sparking and immediate growing at the same temperature as shown in Fig. 2(e), oxides coated on Fe-deposited dots can play only a minor role to control the CNT growing.

3.4. Effect of Au sputtering

Fe was sparked on the Au-sputtered glass slide. Then, CNTs were subsequently grown at 900 K. The result is shown in Fig. 4. It was found that the CNTs can be grown on Fe-deposited dots of the Au-sputtered slide as well.

3.5. Characteristics of the CNT

The CNTs grown at 900 K were put into a beaker containing deionised water. After ultrasonic vibration, the CNT-dispersed water was dropped on a copper grid and dried in ambient atmosphere. By using transmission electron microscopy (TEM), the CNT was studied. TEM and electron diffraction (ED) are shown in Fig. 5. The surface of the CNT is irregular showing that it is not perfect. It contains some defects and disordering atoms. The diameter to thickness ratio of the CNT is 8:1. The ED pattern shows four concentric rings corresponding to (0 0 0 2), (1 0 $\bar{1}$ 1), (0 0 0 4) and (1 1 $\bar{2}$ 0) planes. The strongest ring diffracts from (0 0 0 2) plane. Comparing to the JCPDS [17], the diffraction pattern corresponds to carbon with hexagonal structure. The diffraction rings are diffuse showing that the CNT composes of disordering atoms.

4. Conclusions

No CNTs can be grown on the glass slide without the catalyst. After sparking of Fe on the slides, the CNTs can be grown on the catalytic dots although the temperature is as low as 700 K. Growth rate is increased with an increasing of the temperature. The maximum growth rate is at 900 K. For the present research, carbon with the hexagonal structure was detected. The oxide formation on the catalytic dots can play only a minor role on the CNT growing.

Acknowledgement

The research was supported by The Thailand Research Fund (TRF), Bangkok, Thailand.

References

[1] Y. Shingaya, T. Nakayama, M. Aono, Phys. B 323 (2002) 153–155.
[2] Y. Saito, K. Hata, A. Takakura, J. Yotani, S. Uemura, Phys. B 323 (2002) 30–37.
[3] Y. Homma, T. Yamashita, Y. Kobayashi, T. Ogino, Phys. B 323 (2002) 122–123.
[4] J. Wei, H. Zhu, D. Wu, B. Wei, Appl. Phys. Lett. 84 (2004) 4869–4871.
[5] K. Tsukagoshi, N. Yoneya, S. Uryu, Y. Aoyagi, A. Kanda, Y. Ootuka, B.W. Alphenaar, Phys. B 323 (2002) 107–114.
[6] D. Sarangi, I. Arfaoui, J.M. Bonard, Phys. B 323 (2002) 165–167.
[7] D. Pradhan, M. Sharon, Mater. Sci. Eng. B 96 (2002) 24–28.
[8] Z. Wang, Z. Liang, B. Wang, C. Zhang, L. Kramer, Composites A35 (2004) 1225–1232.
[9] J.I. Sohn, C. Nam, S. Lee, Appl. Surf. Sci. 197–198 (2002) 568–573.
[10] C.J. Lee, J. Park, J.A. Yu, Chem. Phys. Lett. 360 (2002) 250–255.
[11] C.L. Lin, C.F. Chen, S.C. Shi, Diam. Relat. Mater. 13 (2004) 1026–1031.
[12] I. Mukhopadhyay, S. Kawasaki, F. Okino, A. Govindaraj, C.N.R. Rao, H. Touhara, Phys. B 323 (2002) 130–132.
[13] J.C. Bae, Y.J. Yoon, S.J. Lee, H.K. Baik, Phys. B 323 (2002) 168–170.
[14] A.C. Dillon, P.A. Parilla, J.L. Alleman, J.D. Perkins, M.J. Heben, Chem. Phys. Lett. 316 (2000) 13–18.
[15] J.M.C. Moreno, S.S. Swamy, T. Fujino, M. Yoshimura, Chem. Phys. Lett. 329 (2000) 317–322.
[16] G.S. Duesberg, R. Graupner, P. Downes, A. Minett, L. Ley, S. Roth, N. Nicoloso, Synth. Met. 142 (2004) 263–266.
[17] Powder Diffract. File, JCPDS Int. Centre for Diffract. Data, PA 19073-3273, U.S.A., 2001.

Materials Science Forum Vols. 510-511 (2006) pp. 1002-1005
online at http://www.scientific.net

Growth of Carbon Nanorodes on Tungsten Filaments of Light Bulbs

Somchai Thongtem*, Pisith Singjai, Titipun Thongtem and Panumath Saksoangmuang
Faculty of Science, Chiang Mai University, Chiang Mai 50200, Thailand
* Corresponding Author, E-mails : schthongtem@yahoo.com and sthongtem@hotmail.com

Abstract. Carbon nanorodes (CNRs) were grown on the wavy surface of the filaments of light bulbs in 10 $ml.s^{-1}$ Ar containing 0.1 and 0.2 $ml.s^{-1}$ C_2H_2 at a temperature of 900 K. SEM and EDX analyses show locally selective growth of the nanorodes composing of carbon. Selected area electron diffraction (SAED) pattern shows that it is carbon atoms with hexagonal structure. TEM analysis shows the image of CNRs with uneven surface. In addition, electron emission of the CNRs grown on the filaments was measured using applied voltages up to 250 V and the results are in accord with the Fowler-Nordheim equation.

Keywords : Carbon nanorodes, Electron diffraction, Fowler-Nordheim equation

1. Introduction

Since the discovery of carbon nanotubes (CNTs) [1], their properties have been extensively investigated by a number of researchers; especially, their application in electronic technologies; for example, microbattery applications [2], field-emission display [3], cathode ray tube-electron gun [4], the probing tip of a scanning tunneling microscope [5] and the wiring with nanometer diameters and micrometer lengths [6]. The characteristics of CNTs are controlled by several factors such as the surfaces of the substrates [5-7], the catalysts [8&9] and processing temperatures [9]. There are several methods for growing of CNTs; for example, arc discharge [10], laser ablation [11], electrophoresis [12], arc-water method [13] and thermal chemical vapor deposition [14-16]. For the present research, a simple equipment has been used for growing carbon nanorodes (CNRs) on the wavy surface of the tungsten filaments of light bulbs without any additional catalysts in the atmosphere containing carbon at high temperature. Then, the characteristics and properties of the CNRs were intensively discussed.

2. Experiment

Argon and acetylene used for the process were purified by flowing through glass columns containing anhydrous calcium sulfate and Ascarite^{TM} for water vapor and oxides of carbon removal, respectively. Flow rates of the purified gases were controlled using venturi meters.

The wavy surface of the filament of a light bulb (12 V, 21 W) was used as a substrate. It was dipped in 48 % HF for 5 s, rinsed with distilled water and dried in an ambient atmosphere. No catalyst was used in this process. It was then hung in a high temperature reaction chamber which was made of high alumina porcelain and fired at 1,573 K. The water cooled copper cap was tightly closed on top of the chamber and the air was replaced by the 10 $ml.s^{-1}$ Ar for 600 s. The filament was then heated in the flowing Ar until the temperature reached 900 K. The additional 0.1 or 0.2 $ml.s^{-1}$ C_2H_2 was fed into the chamber. The process proceeded for 300 s. At the conclusion of the process, the acetylene was turned off and the filament was cooled down in the Ar to room temperature. Emission current was measured at the applied voltage between the copper anode (3.14 cm^2) and CNRs cathode of 0-250 V in 10^{-6} Torr vacuum. The anode-cathode gap was 2.0 mm. In addition, the filaments and CNRs were analyzed using a SEM equipped with an EDX operated at 15 kV and a TEM operated at 200 kV.

3. Results and Discussion

3.1 SEM and EDX

Different positions on the filaments before and after process in 10 $ml.s^{-1}$ Ar containing 0.1 and 0.2 $ml.s^{-1}$ C_2H_2 were analyzed using SEM and EDX. Before processing, the substrate is a wavy surface and tungsten was detected. After processing, SEM and EDX are shown in Fig 1. The maximum growth rate of the CNRs was increased by one order of magnitude when the acetylene flow rate was raised from 0.1 to 0.2 $ml.s^{-1}$. There are a number of CNRs grown in different directions with sizes less than 100 nm in diameter and up to 3.6 μm in length. Their shapes are both bent and straight. The formation of the CNRs was root growth mechanism and locally

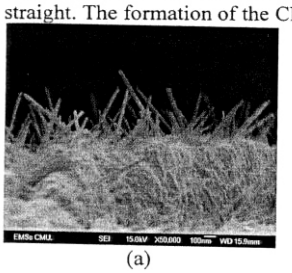

(a)

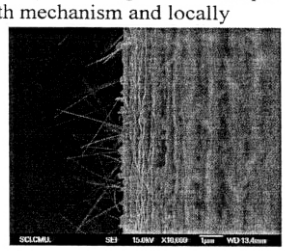

(b)

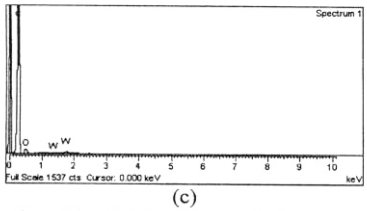

(c)

Fig 1. SEM of the CNRs grown in Ar containing (a) 0.1 $ml.s^{-1}$ C_2H_2 and (b) 0.2 $ml.s^{-1}$ C_2H_2. (c) EDX of the CNR grown in Ar containing 0.2 $ml.s^{-1}$ C_2H_2.

selective. The EDX point analysis on the CNR shows the existence of carbon containing oxygen and a small amount of tungsten. During growing the CNRs, the oxygen is likely to be from the following :- (1). The impurity contained in the argon gas. (2). The oxygen left in the chamber during preheating. (3). The reduction of silica contained in the high alumina porcelain chamber by the hydrogen from acetylene.

During the EDX point analysis, the diameter of the electron beam is larger than that of the CNR leading to the unexpected oxygen and tungsten peaks. Tungsten and oxygen may condense to be tungsten oxide(s). According to the vapor-liquid-solid mechanism, it is likely that tungsten sub-oxide provided the liquid-solid seeds working as catalytic particles [17]. The characteristics, impurities and selective growth of the CNRs are the factors that control the emission current.

3.2 Field-Emission

The relationships between the emission current (I) and the applied voltage (V) of the substrate composing of the CNRs were determined. The relationships between $\ln(I/V^2)$ and $(1/V)$ are shown in Fig 2. The data points are in agreement with the Fowler-Nordheim equation [18-22]. The plots show that the emission current is controlled by the C_2H_2 flow rate, the number of CNRs per unit surface area, the characteristics of the CNRs and others. The electrons may emit from the tip of the CNRs and the wavy surface of the tungsten filaments depending on their work functions, conductivities, perfection of the CNRs and others. The emission current is increased with the increase of the applied voltage. At an applied voltage of 50 V(electric field intensity of 0.025 $V.\mu m^{-1}$) , the least emission current values for 0.1 and

0.2 ml.s^{-1} C_2H_2 are 0.3 and 0.2 μA, respectively. In addition, the field emission of CNRs grown on the tungsten filament of light bulbs was measured by increasing the applied voltage from 0 to 250 V and decreasing the voltage to the starting condition. It was found that the behavior of the emission is reproducible.

3.3 SAED and TEM

The CNRs were put into a beaker containing deionized water. After ultrasonic vibration, the CNR-dispersed water was dropped on a copper grid and dried in ambient atmosphere. The selected area electron diffraction (SAED) and TEM of the CNRs were analyzed and the results are shown in Fig 3. The diffraction pattern was interpreted [23]. The pattern diffracting from the $(10\bar{2})$, $(\bar{1}0\bar{2})$, $(1\bar{1}0)$, $(\bar{1}10)$ and $(0\bar{1}\bar{2})$ planes appears as a hexagonal arrangement of carbon atoms. The farthermost spot diffracting from the $(\bar{1}\bar{1}\bar{4})$ plane is also shown. The calculated angles between any pair of the directions are in accord with those of the diffraction patterns on the film. With the exception of the $(1\bar{1}0)$ and $(\bar{1}10)$ planes, the values of d-spacing determined from the (hkl) are in accord with those determined from the diffracted pattern on the film. The incident beam of electron might not be exactly perpendicular to the graphite plane leading to the asymmetric diffraction pattern. In addition, zone axis is in the $[22\bar{1}]$ direction which is parallel or nearly parallel to the electron beam.

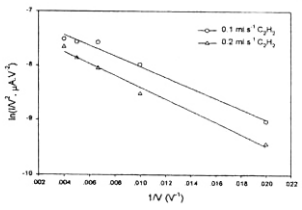

Fig 2. Fowler-Nordheim plots of the CNRs grown in Ar containing 0.1 and 0.2 ml.s^{-1} C_2H_2.

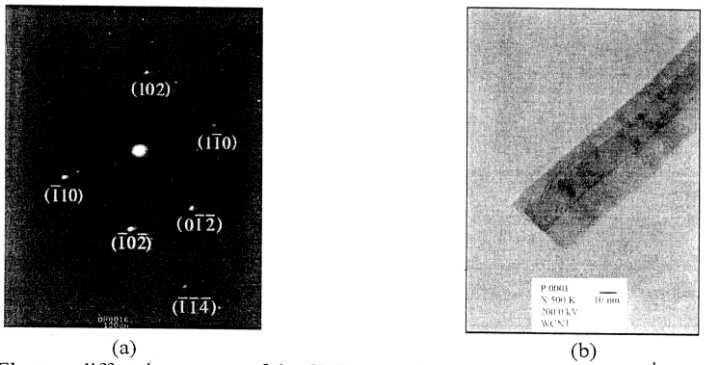

(a) (b)

Fig 3. (a) Electron diffraction pattern of the CNR grown in Ar containing 0.2 ml.s^{-1} C_2H_2. (b) TEM of the selected CNRs grown in Ar containing 0.1 ml.s^{-1} C_2H_2.

TEM of the selected grown CNRs shows dark and light contrast bands without holes inside. They are likely to be two rods with 18 and 43 nm diameter and one rod overlapping the other. However, the dark and light contrast bands can be two rods with 26 and 35 nm diameter and

some part of one rod covering some part of the other. The external surface of the rod is not even showing that the formation of the carbon network is not perfect.

4. Conclusions

The CNRs were successfully grown on the wavy surface of the tungsten filament of a light bulb in flowing Ar containing C_2H_2 and were root growth in combination with locally selective. The arrangement of carbon atoms is a hexagonal structure, but is not perfect. The behavior of the electron field emission is in agreement with the Fowler-Nordheim equation.

Acknowledgement

The research was supported by The Thailand Research Fund, Bangkok, Thailand.

References

1. S. Iijima, Nature, 354(1991)56.
2. Z. Zhang, C. Dewan, S. Kothari, S. Mitra and D. Teeters, Mater. Sci. Engineer. B, 116(2005)363.
3. W.B. Choi, D.S. Chung, J.H. Kang, H.Y. Kim, Y.M. Jin, I.T. Han, Y.H. Lee, J.E. Jung, N.S. Lee, G.S. Park and J.M. Kim, Appl. Phys. Lett., 75(1999)3129.
4. Y.T. Jang, Y.H. Lee, B.K. Ju, J.H. Ahn, C.K. Go and G.S. Park, Vacuum, 68(2003)79.
5. Y. Shingaya, T. Nakayama and M. Aono, Physica B, 323(2002)153.
6. Y. Homma, T. Yamashita, Y. Kobayashi and T. Ogino, Physica B, 323(2002)122.
7. O. Noury, T. Stöckli, M. Croci, A. Châtelain and J.M. Bonard, Chem. Phys. Lett., 346(2001)349.
8. D.S. Bethune, Physica B, 323(2002)90.
9. O.A. Nerushev, R.E. Morjan, D.I. Ostrovskii, M. Sveningsson, M. Jönsson, F. Rohmund and E.E.B. Campbell, Physica B, 323(2002)51.
10. I. Mukhopadhyay, S. Kawasaki, F. Okino, A. Govindaraj, C.N.R. Rao and H. Touhara, Physica B, 323(2002)130.
11. H. Shimoda, L. Fleming, K. Horton and O. Zhou, Physica B, 323(2002)135.
12. J.C. Bae, Y.J. Yoon, S.J. Lee and H.K. Baik, Physica B, 323(2002)168.
13. L.A. Montoro, R.C.Z. Lofrano and J.M. Rosolen, Carbon, 43(2005)200.
14. D. Sarangi, I. Arfaoui and J.M. Bonard, Physica B, 323(2002)165.
15. C.J. Lee and J. Park, Appl. Phys. Lett., 77(2000)3397.
16. T. Ikuno, T. Yamamoto, M. Kamizono, S. Takahashi, H. Furuta, S.I. Honda, S. Ohkura, M. Katayama, T. Hirao and K. Oura, Physica B, 323(2002)171.
17. C.J. Lee, S.C. Lyu, H.W. Kim, J.W. Park, H.M. Jung and J. Park, Chem. Phys. Lett., 361(2002)469.
18. S. Honda, Y.G. Baek, K.Y. Lee, T. Ikuno, T. Kuzuoka, J.T. Ryu, S. Ohkura, M. Katayama, K. Aoki, T. Hirao and K. Oura, Thin Solid Films, 464-465(2004)290.
19. G.N. Fursey, D.V. Novikov, G.A. Dyuzhev, A.V. Kotcheryzhenkov and P.O. Vassiliev, Appl. Surf. Sci., 215(2003)135.
20. Y.M. Wong, S. Wei, W.P. Kang, J.L. Davidson, W. Hofmeister, J.H. Huang and Y. Cui, Diam. Relat. Mater., 13(2004)2105.
21. O.A. Nerushev, M. Sveningsson, L.K.L. Falk and F. Rohmund, J. Mater. Chem., 11(2001)1122.
22. Y. Chen, S.Z. Deng, N.S. Xu, J. Chen, X.C. Ma and E.G. Wang, Mater. Sci. Engineer. A, 327(2002)16.
23. K.W. Andrews, D.J. Dyson and S.R. Keown, (Interpret. Electr. Diffract. Patter., 2nd ed, Plenum Press, NY, 1971).

ISSN 0020-1685, Inorganic Materials, 2007, Vol. 43, No. 2, pp. 143–147. © Pleiades Publishing, Inc., 2007.

Synthesis of CNTs via Ethanol Decomposition over Ball-Milled Fe_2O_3 Coated Copper Sheets[1]

P. Singjai[a], T. Thongtem[b], S. Kumfu[a], and S. Thongtem[a]

[a] *Department of Physics, Faculty of Science, Chiang Mai University, Chiang Mai, 50200 Thailand*

[b] *Department of Chemistry, Faculty of Science, Chiang Mai University, Chiang Mai, 50200 Thailand*

e-mail: schthongtem@yahoo.com, sthongtem@hotmail.com

Received March 22, 2006; in final form, July 14, 2006

Abstract—Carbon nanotubes (CNTs) were synthesized on ball-milled Fe_2O_3 coated copper sheets by the catalytic decomposition of ethanol vapor at 650°C. TEM, SEM, and EDX revealed the presence of 30–50 nm diameter multiwalled carbon nanotubes with catalytic particles at their tips. CNTs, α-Fe, and Fe_3C were detected by XRD. Raman and TG analyses show that the product is CNTs with less than 10 wt % residues. The carbon yield was the maximum at 354 wt %.

DOI: 10.1134/S0020168507020094

INTRODUCTION

Since the discovery of multiwalled carbon nanotubes (MWNTs) by Iijima in 1991 [1], synthetic methods have been widely investigated such as arc-discharge [2], chemical vapor deposition (CVD) [3], and laser vaporization [4]. To exploit their chemical and mechanical properties for industrial purposes, large-scale synthesis and low cost are necessary. Among these, CVD has shown to be suitable for scaling up carbon nanotubes (CNTs) [5–9]. To synthesize CNTs, a number of powders were used such as Al_2O_3 [5], MgO [6], and zeolite [9–12]. The flat substrates were silicon [13, 14], aluminum [15, 16], and copper [17]. For the present research, large-scale CNTs were synthesized by ethanol vapor decomposition over ball-milled iron oxide coated copper sheets.

EXPERIMENTAL

A mixture of ball-milled Fe_2O_3 powder and ethanol was applied to 60×170 mm^2 copper sheets. Each sheet was rolled and put in a tube furnace, as shown in Fig. 1. The sheet was heated up in argon until the test temperature was 650°C. Then ethanol vapor was supplied to the sheet using 10 ml/s bubbling argon. At the end of the process, the furnace was turned off. The copper sheet was left to cool to room temperature in argon. By using HCl (1 M) for treatment, black powder was obtained on the sheet. The product was analyzed using a scanning electron microscope (SEM) equipped with an energy dispersive x-ray (EDX) analyzer, an x-ray diffractometer (XRD) combined with JCPDS software [18], a transmission electron microscope (TEM), a thermogravimetric analyzer (TGA), and a Raman spectrometer. The carbon yield was estimated using the equation:

$$\text{Carbon yield (wt\%)} = W_{CNTs}/W_C \times 100,$$

where W_{CNTs} is the weight of the as-grown CNTs, without the catalyst, and W_C is the approximate weight of the catalyst.

RESULTS AND DISCUSSION

A TEM image of the product is shown in Fig. 2. Multiwalls were clearly detected. External and internal surfaces are rough due to the presence of oxygen and water vapor from the ethanol decomposition. The product is composed of some disordering atoms. Generally, roughness is the surface property to enhance mechanical interlocking between the tubes and the matrix for reinforcement of composite materials.

Some catalytic particles were detected at the tips and indicated by arrows in Fig. 3. This shows that a tip growth mode is dominant. The diameters are in the range 30–50 nm. CNTs were also synthesized using as-received Fe_2O_3 powder (results not shown). Their diameters were 100–300 nm. Ball milling can induce stresses and cracks in Fe_2O_3 powder, which acts as a nanosized catalyst and influences the CNT diameter. A 80 ml of CNTs synthesized by a single batch is shown in the beaker. EDX analysis shows that the atomic per-

[1] The text was submitted by the authors in English.

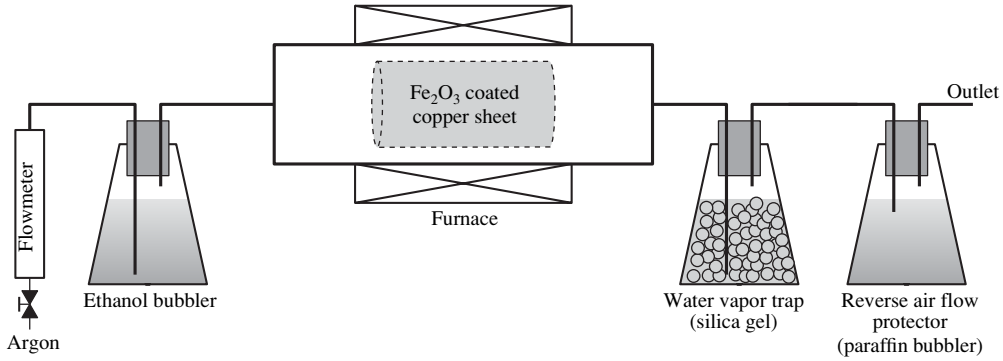

Fig. 1. Schematic diagram of CNT synthesis.

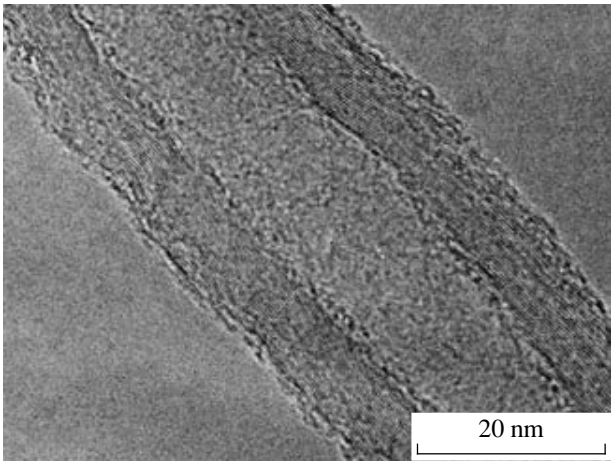

Fig. 2. TEM image of the as-grown product synthesized by flowing ethanol vapor and argon over a ball-milled Fe_2O_3 coated copper sheet.

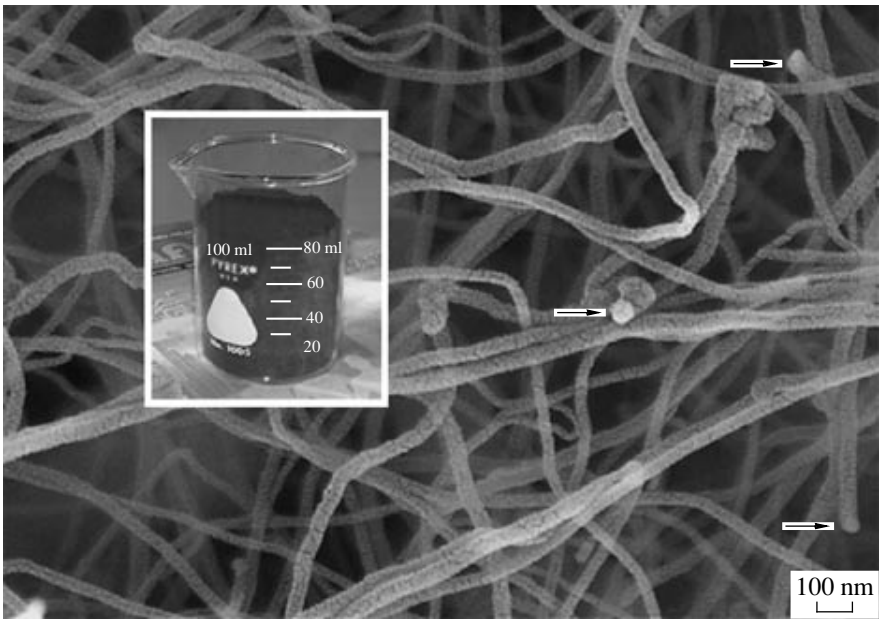

Fig. 3. SEM image of the as-grown product with 80 ml CNTs synthesized by a single batch.

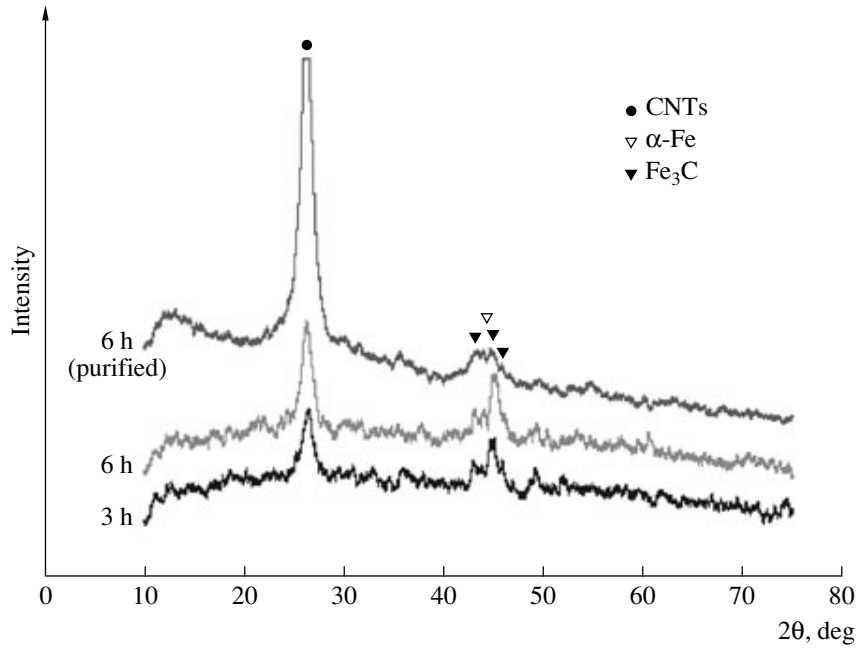

Fig. 4. XRD spectra of as-grown and purified products synthesized for a variety of reaction times.

centages of carbon, oxygen, and iron are 97, 2.5, and 0.5, respectively.

The XRD spectra of the as-grown and purified products are shown in Fig. 4. Peaks of CNTs, α-Fe, and Fe_3C were detected. This shows that Fe_2O_3 reacted with ethanol to form Fe and Fe_3C. The strongest peak of the CNTs diffracting from the 002 plane is at 26.2°. Comparing between the as-grown and purified products, the XRD intensity of the latter is the highest. The presence of α-Fe and Fe_3C peaks is in accord with the SEM detection of catalytic particles at the tips. These show that CNTs grew by the decomposition of Fe_3C into Fe and graphite [18].

The Raman spectrum of the as-grown CNTs analyzed using the 488 nm excitation wavelength is shown in Fig. 5. The D and G bands were detected at 1344 and

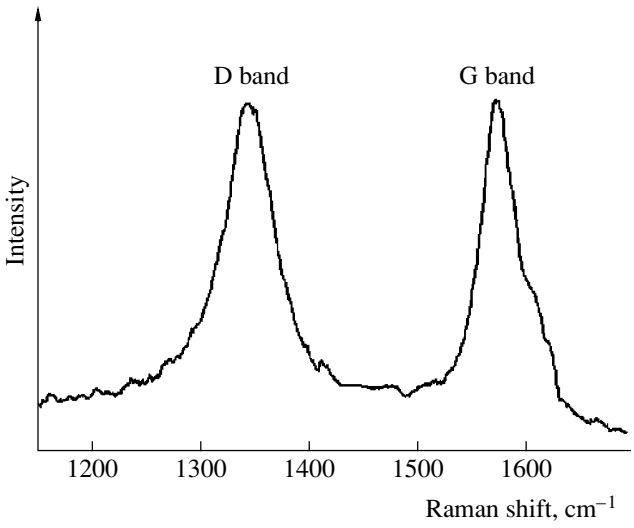

Fig. 5. Raman spectrum (488-nm excitation wavelength) of as-grown CNTs.

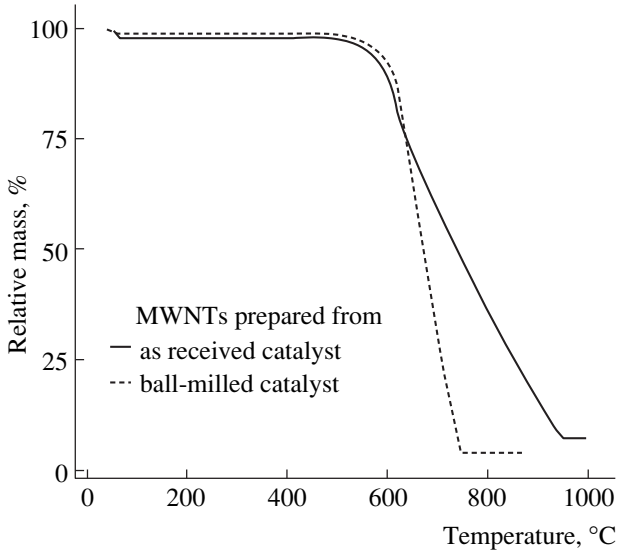

Fig. 6. TGA curves of as-grown CNTs or MWNTs synthesized on as-received and ball-milled Fe_2O_3 powders.

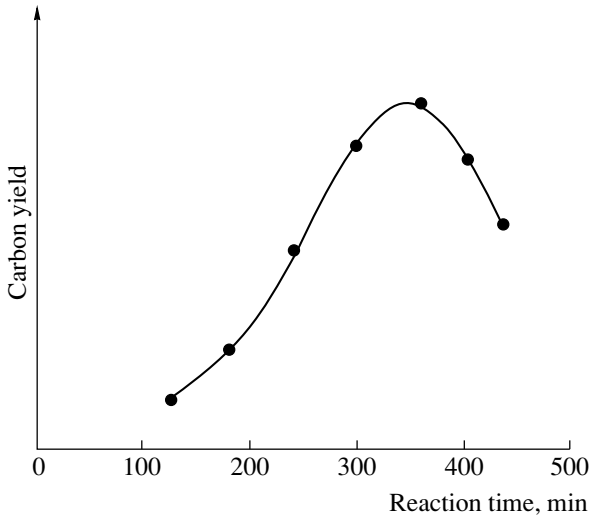

Fig. 7. Carbon yield as a function of reaction time.

1572 cm^{-1}, respectively. The intensities of the two peaks are almost equal due to the effect of surface roughness and the small amount of the amorphous phase in the product.

The TGA curves of CNTs or MWNTs synthesized on the as-received (A) and ball-milled (B) Fe_2O_3 powders are shown in Fig. 6. The curves for the A-CNTs and B-CNTs show weight losses over the range of 497–953 and 497–741°C due to carbon evaporation. The above explanation shows that the A-CNTs are larger than the B-CNTs. Therefore, the oxidation or evaporation rate of the A-CNTs is less than that of the B-CNTs. Above 953°C for the A-CNTs and 741°C for the B-CNTs, weights are constant. The total weight losses are 90.4 and 93.5 wt %, respectively.

The carbon yield of the B-CNTs using 1.0 g ball-milled Fe_2O_3 as a function of the reaction time is shown in Fig. 7. The carbon yield increased to the maximum value of 354 wt % (3.18 g as-grown CNTs) in 6 h. The optimum yield is in accord with the maximum XRD intensity of purified CNTs at 6 h as well. At longer reaction times, the carbon yield decreased slowly due to the decrease in catalytic activity.

CONCLUSIONS

CNTs were successfully synthesized by the catalytic decomposition of ethanol vapor over Fe_2O_3 powder on copper sheets. They grew by a tip growth mechanism and were multiwalled. Fe_2O_3 powder was transformed into Fe and Fe_3C nanosized particles. The maximum carbon yield was 354 wt % (3.18 g as-grown CNTs) at 6 h, in accord with the maximum XRD intensity of the purified CNTs synthesized over the same reaction time. TGA showed weight losses due to carbon evaporation.

ACKNOWLEDGMENTS

This research was supported by the Thailand Research Fund and the Commission on Higher Education, Bangkok, Thailand.

REFERENCES

1. Iijima, S., Helical Microtubules of Graphitic Carbon, *Nature*, 1991, vol. 354, pp. 56–58.
2. Journet, C., Maser, W.K., Bernier, P., et al., Large-Scale Production of Single-Walled Carbon Nanotubes by the Electric-Arc Technique, *Nature*, 1997, vol. 388, pp. 756–758.
3. Park, J.B., Choi, G.S., Cho, Y.S., et al., Characterization of Fe-Catalyzed Carbon Nanotubes Grown by Thermal Chemical Vapor Deposition, *J. Cryst. Growth*, 2002, vol. 244, pp. 211–217.
4. Guo, T., Nikolaev, P., Thess, A., et al., Catalytic Growth of Single-Walled Nanotubes by Laser Vaporization, *Chem. Phys. Lett.*, 1995, vol. 243, pp. 49–54.
5. Gulino, G., Vieira, R., Amadou, J., et al., C_2H_6 as an Active Carbon Source for a Large Scale Synthesis of Carbon Nanotubes by Chemical Vapour Deposition, *Appl. Catal., A*, 2005, vol. 279, pp. 89–97.
6. Li, Y., Zhang, X.B., Tao, X.Y., et al., Mass Production of High-Quality Multi-walled Carbon Nanotube Bundles on a Ni/Mo/MgO Catalyst, *Carbon*, 2005, vol. 43, pp. 295–301.
7. Singh, C., Shaffer, M.S.P., Koziol, K.K.K., et al., Towards the Production of Large-Scale Aligned Carbon Nanotubes, *Chem. Phys. Lett.,* 2003 vol. 372, pp. 860–865.
8. Hou, H., Schaper, A.K., Jun, Z., et al., Large-Scale Synthesis of Aligned Carbon Nanotubes Using $FeCl_3$ as Floating Catalyst Precursor, *Chem. Mater.*, 2003, vol. 15, pp. 580–585.
9. Maruyama, S., Kojima, R., Miyauchi, Y., et al., Low-Temperature Synthesis of High-Purity Single-Walled Carbon Nanotubes from Alcohol, *Chem. Phys. Lett.,* 2002, vol. 360, pp. 229–234.
10. Okazaki, T. and Shinohara, H., Synthesis and Characterization of Single-Wall Carbon Nanotubes by Hot-Filament Assisted Chemical Vapor Deposition, *Chem. Phys. Lett.*, 2003, vol. 376, pp. 606–611.
11. Chiashi, S., Murmaki, Y., Miyauchi, Y., and Maruyama, S., Cold Wall CVD Generation of Single-Walled Carbon Nanotubes and In Situ Raman Scattering Measurements of the Growth Stage, *Chem. Phys. Lett.*, 2004, vol. 386, pp. 89–94.

12. Okamoto, A. and Shinohara, H., Control of Diameter Distribution of Single-Walled Carbon Nanotubes Using the Zeolite-CCVD Method at Atmospheric Pressure, *Carbon*, 2005, vol. 43, pp. 431–436.
13. Emmenegger, C., Mauron, P., Zuttel, A., et al., Carbon Nanotube Synthesized on Metallic Substrates, *Appl. Surf. Sci.*, 2000, vols. 162–163, pp. 452–456.
14. Mauron, P., Emmenegger, C., Zuttel, A., et al., Synthesis of Oriented Nanotube Films by Chemical Vapor Deposition, *Carbon*, 2002, vol. 40, pp. 1339–1344.
15. Hongo, H., Nihey, F., Ichihashi, T., et al., Support Materials Based on Converted Aluminum Films for Chemical Vapor Deposition Growth of Single-Wall Carbon Nanotubes, *Chem. Phys. Lett.*, 2003, vol. 380, pp. 158–164.
16. Emmenegger, C., Bonard, J.M., Mauron, P., et al., Synthesis of Carbon Nanotubes over Fe Catalyst on Aluminium and Suggested Growth Mechanism, *Carbon,* 2003, vol. 41, pp. 539–547.
17. Volkova, E.G., Volkov, A.Y., Murzakaev, A.M., et al., Carbon Nanostructures Synthesized at Metallic Foils, *Phys. Met. Metallogr.,* 2003, vol. 95, pp. 342–345.
18. *Powder Diffraction File,* Newtown Square: ICDD, 2001.

ELSEVIER

Materials Science and Engineering A 443 (2007) 42–46

MATERIALS SCIENCE & ENGINEERING A

www.elsevier.com/locate/msea

Electrical resistivity of bulk multi-walled carbon nanotubes synthesized by an infusion chemical vapor deposition method

P. Singjai *, S. Changsarn, S. Thongtem

Nanomaterials Research Unit, Department of Physics, Faculty of Science, Chiang Mai University, Chiang Mai 50200, Thailand

Received 17 April 2006; received in revised form 10 June 2006; accepted 17 June 2006

Abstract

Multi-walled carbon nanotubes (MWNTs) were synthesized by infusing alcohol into a tube furnace. A nickel catalyst preparation was made by a reduction reaction of NiO powder by ethanol vapor at 450 °C for 30 min before the MWNT synthesis at 700 °C for 1–18 h. The as-grown MWNTs were characterized by scanning electron microscopy, transmission electron microscopy, X-ray diffraction and Raman spectroscopy. Large quantities of MWNTs, having a diameter in the range of 20–50 nm can be produced from ethanol vapor without a carrier gas by this technique. A method to measure an electrical resistance of bulk MWNTs was carried out under stress between two conducting plates. The result shows an exponentially correlation between the resistivity and the D-band/G-band intensity ratio, suggesting that the measuring method provides a simple tool to monitor the degree of structural defects of MWNTs.

Keywords: Carbon nanotubes; Chemical vapor deposition; Electrical resistivity

1. Introduction

Since the discovery of carbon nanotubes (CNTs) by Iijima [1], the field has been developed rapidly because of their unique electronic and mechanical properties. Depending on the detailed atomic structure they are either metallic or semiconducting, as well as a very large Young's modulus in their axial direction [2]. Thus, there are many potential applications of CNTs, such as reinforcement in composite materials [3], hydrogen storage for fuel cells [4,5], electrodes in batteries and capacitors [6,7], field emitting devices [8–10], probe tips for scanning probe microscope (SPM) [11] and gas-sensing devices [12,13].

CNTs can be synthesized by various techniques such as arc discharge, laser ablation and chemical vapor deposition (CVD) [14,15]. Among these synthesis methods, the CVD has shown to be the most potential method to scale up CNTs at a low cost [16–20]. Ethanol, known as a very promising candidate of a low raw material cost by using alcohol catalytic CVD (AC-CVD) was reported by Maruyama et al. [20]. From these facts, several research groups have used ethanol as the carbon source to produce single-walled carbon nanotubes (SWNTs) [20–24] and MWNTs [25,26] by various CVD methods such as thermal CVD [20], hot-filament CVD [21], cold-wall CVD [22,23] and pulsed laser vaporization [24].

There are some technical difficulties of electrical resistivity measurements on an individual CNT as well as the results are very sample-dependent [27,28]. Thus, Ma et al. [29] have investigated an electrical conductivity of hot-pressed sintered CNTs. The electrical properties and the associated measurement techniques of bulk, bundles or ropes of CNTs provide an alternative approach to study a macroscopic scale of both basic science and applications of CNTs [29,30]. In this work, MWNTs have been synthesized by an infusion CVD method using ethanol as the carbon source. The method to measure electrical resistivity of the bulk MWNTs at room temperature has been demonstrated to monitor the degree of their structural defects.

2. Experimental

A schematic view of the infusion CVD apparatus is shown in Fig. 1. The experiment started with a valve-controlled gravity flow of infusing 0.2 ml/min ethanol into a tube furnace containing 0.5 g nickel oxide powder. The ethanol was then evaporated at its boiling temperature to a vapor form at a

* Corresponding author. Tel.: +66 53 941922x610; fax: +66 53 892271.
E-mail address: singjai@chiangmai.ac.th (P. Singjai).

0921-5093/$ – see front matter © 2006 Elsevier B.V. All rights reserved.
doi:10.1016/j.msea.2006.06.042

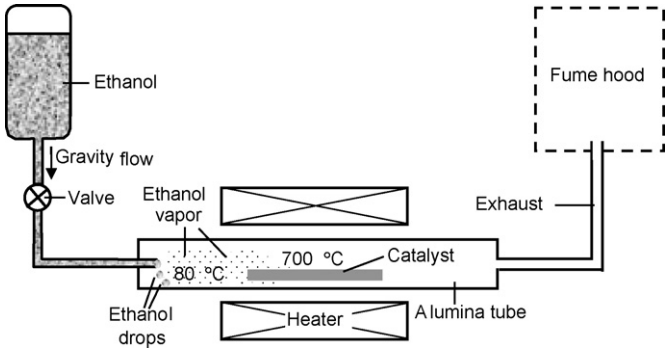

Fig. 1. Schematic diagram of the infusion CVD apparatus.

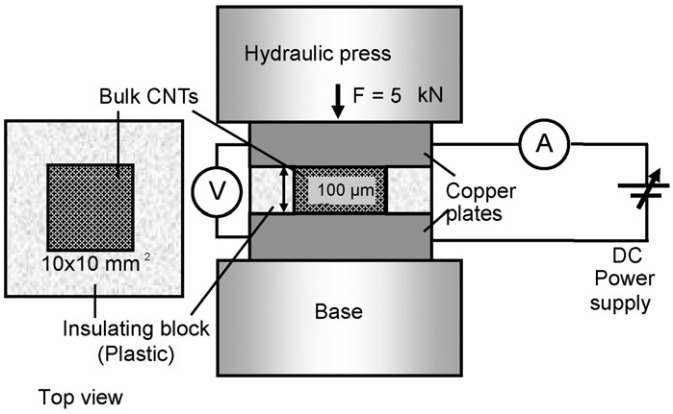

Fig. 2. Schematic diagram of the electrical resistance measurement.

pressure in which the ethanol vapor-flowing tube furnace was occurred. Nickel oxide was reduced by the ethanol vapor at 450 °C for 30 min before the MWNTs were synthesized at 700 °C for 1–18 h. The structure, morphology and quality of the as-prepared product were characterized by using scanning electron microscopy (SEM, JEOL JSM-6335F), transmission electron microscopy (TEM, JEOL JEM-2010), X-ray Diffractometer (XRD, Bruker D8 Advance) and Raman spectroscopy (HORIBA JOBIN YVON T64000). An experimental set-up for the electrical resistance measurement of the as-grown sample is shown in Fig. 2. The amount of 20 mg MWNTs was placed into the insulating block area of 10 mm × 10 mm and thickness of 100 μm, estimated from an assumed microscopic density of 2.0 g/cm^3. The measurements were carried out under the compressive stress of 3 MPa between two copper plates to obtain *I–V* curves of the MWNTs and a known sample (graphite powder, Sigma–Aldrich, −325 mesh, purity >99.99%).

3. Results and discussion

SEM image of the as-grown MWNTs (6 h) is shown in Fig. 3, given the tube diameter in the range of 20–50 nm with the average size of approximately 27 nm and the length of greater than 10 μm. It is noted that a contrast between the tube center and the tube wall of an individual MWNT is apparently seen as well as some bright patches of their cross-sectional orientations. However, some bright particles of Ni catalyst were barely observed

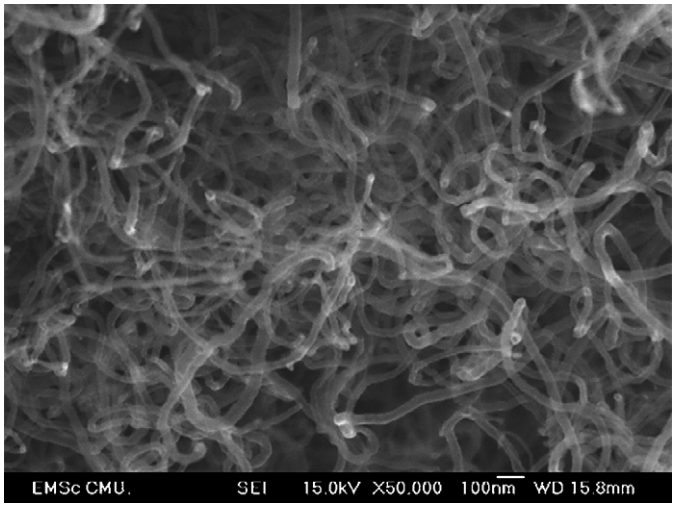

Fig. 3. SEM image of the as-grown MWNTs at the synthesis time of 6 h.

which resulted from a high MWNT to catalyst weight ratio and a high growth rate (1.34 g/h).

Fig. 4 shows the XRD patterns of the as-grown MWNTs (1–18 h). The peak at 26.2° comes from carbon and the small peaks at 44.5°, 51.8° and 76.4° correspond to the FCC structure of the Ni catalyst. The MWNT peak increased with the synthesis time whereas those of nickel decreased, suggesting that the XRD result is in good agreement with the SEM image. Furthermore, the broad MWNT peak, especially from the 18 h synthesized sample reveals greater structural defects.

TEM image and (inset) the associated selected area electron diffraction pattern (SADP) of an individual MWNT are shown in Fig. 5. The fringes of graphite layers show the MWNT structure with some degree of disorder and defects. The hexagonal structure of MWNTs has been confirmed by the corresponding crystallographic (0 0 2), (1 0 1), (0 0 4) and (1 1 0) planes.

Fig. 6 shows Raman spectra of the as-grown MWNTs and the three Lorentzian peak fits at the synthesis times of 1–18 h. The

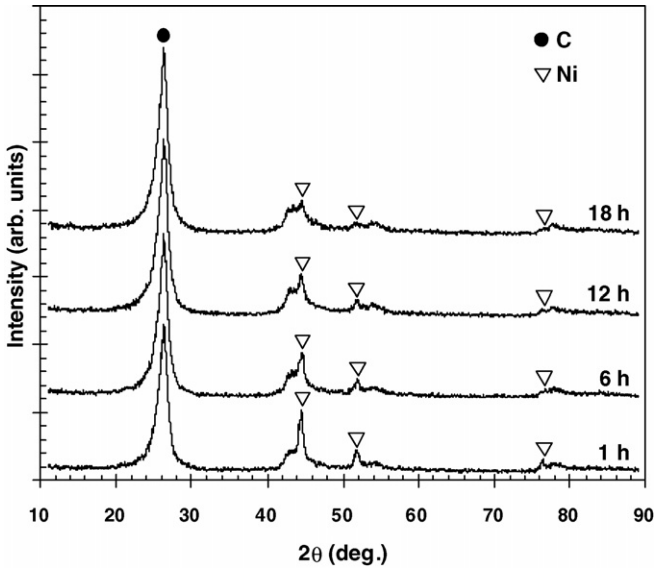

Fig. 4. XRD patterns of as-grown MWNTs at the synthesis times of 1–18 h.

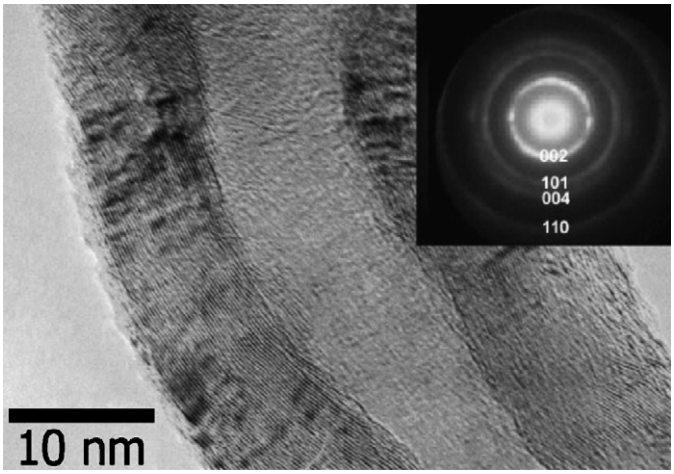

Fig. 5. TEM image and the associated SADP of an individual MWNT.

Table 1
Fits to the Raman spectra for the as-grown MWNTs (1–18 h) including three Lorentzians for each spectrum

Synthesis time (h)	D-band (cm^{-1})	G-band (cm^{-1})	Shoulder (cm^{-1})	I_D/I_G	I_S/I_D
1	1349	1575	1604	0.84	0.21
6	1351	1578	1606	0.90	0.21
12	1349	1573	1604	1.17	0.22
18	1348	1577	1606	2.37	0.27

three Lorentzian peak fits indicate the peak centers at approximately 1349, 1576 and 1605 cm^{-1} which are the disorder-induced vibrational mode (D-band), the in-plane carbon stretching mode (G-band) and the G-band shoulder (I_S) associated with structural defects [31], respectively. The D-band/G-band intensity ratio (I_D/I_G) increased with the synthesis time whereas the I_S/I_D ratio was considered to be unchanged (see Table 1).

Bulk resistance of MWNTs as the Ohmic *I–V* characteristic is shown in Fig. 7. It is clearly seen that the resistance

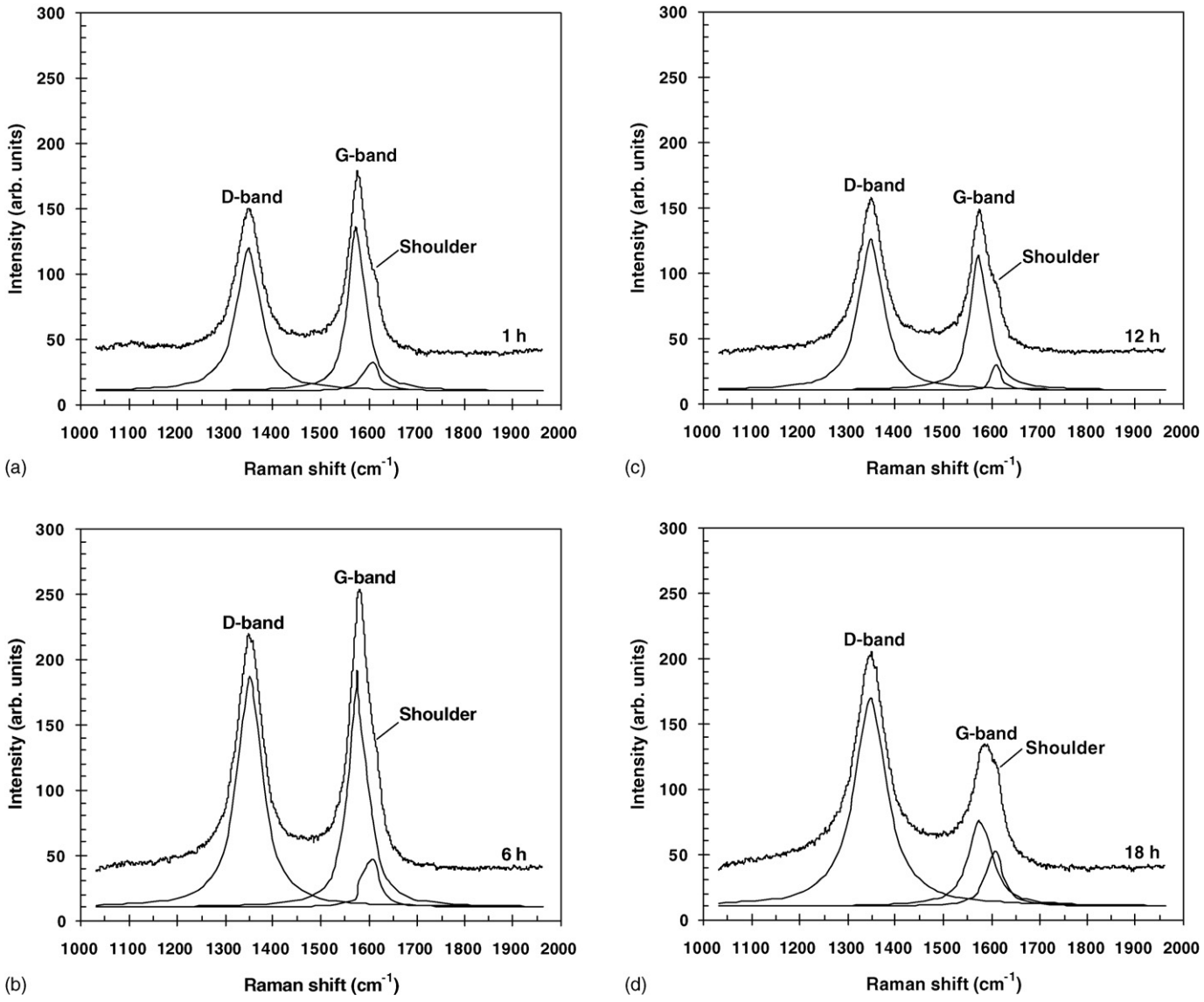

Fig. 6. Raman spectra of the as-grown MWNTs and the three Lorentzian peak fits at the synthesis times of (a) 1 h, (b) 6 h, (c) 12 h and (d) 18 h.

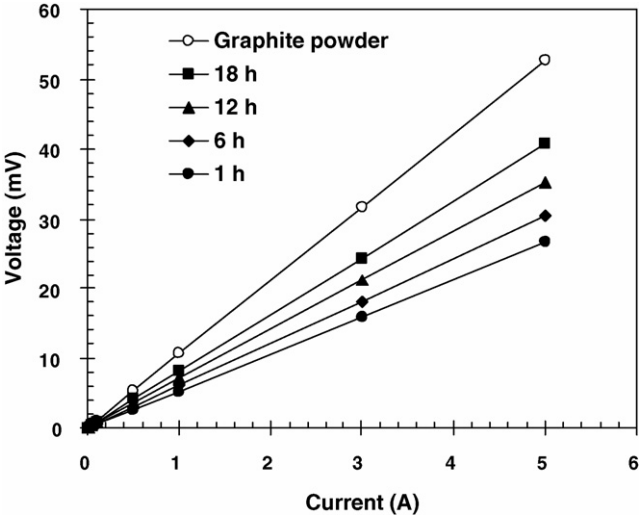

Fig. 7. *I–V* curves of the as-grown MWNTs and the graphite powder as a known sample.

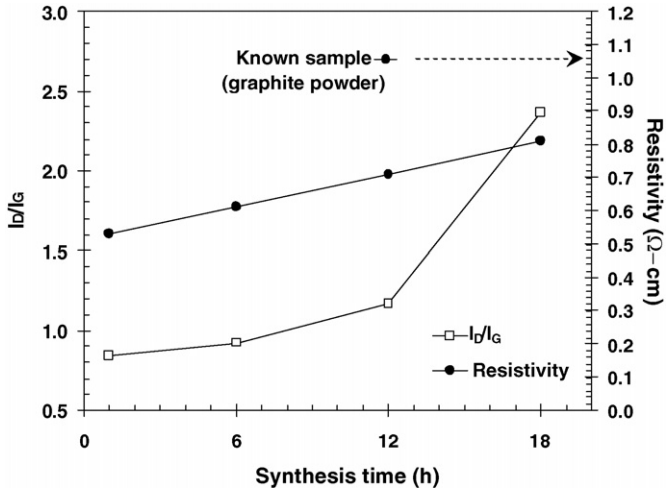

Fig. 8. Comparison of the I_D/I_G ratio as the degree of structural defects and the electrical resistivity of as-grown MWNTs.

increases linearly with the synthesis time. The lowest resistivity was estimated to be 0.53 Ω cm at the synthesis time of 1 h whereas that of graphite powder as a known sample was twice, i.e. 1.06 Ω cm. It should be noted that these measurements are highly repeatable and precise from run to run, i.e. with an error from the mean resistivity of less than 1%. However, the resistivity of the MWNTs measured by this technique was three orders of magnitude greater than that of the hot-pressed sintered CNTs (10^{-4} Ω cm) [29]. This can be attributed by the poor inter-tube contacts [30], which resulted from the relatively low compressive stress between two copper plates. Comparisons between bulk MWNT resistivities, measured at room temperature by this technique and by others are summarized in Table 2 [32,33]. As discussed above, the resistivity of bulk CNTs may depend on the measuring condition, however, our measuring method is a relatively simple tool to quantify a resistivity of bulk CNTs.

Fig. 8 shows a comparison of the I_D/I_G ratio and the resistivity of the as-grown MWNTs, the exponentially correlation was observed. The result has been demonstrated that the more synthesis time (>1 h) by this present method, the more structural defects of CNTs were observed. A possible explanation was given that the as-grown CNTs were degraded by an accumulative amount of the decomposed OH radicals. Since, the too-high amount of such an oxidizer in the reactor would also attack the ordered carbon in the form of CNTs at the high temperature [20,34].

Table 2
Comparisons between bulk resistivities of MWNTs, measured at room temperature by this technique and by some previous works

Result from	Measuring condition	Resistivity (Ω cm)
This work	CNTs under stress between two conducting plates	$(5–8) \times 10^{-1}$
Ma et al. [29]	Hot-pressed sintered CNTs	$(2–3) \times 10^{-4}$
Li et al. [32]	Four-point method of CNT ribbons	$(4.4–12.6) \times 10^{-4}$
Qin et al. [33]	Four-point method of sintered CNTs compact	$(1.2–1.6) \times 10^{-2}$

Detailed insights into the mechanism of the CNT growth from ethanol were preliminary discussed, for example in the case of SWNTs by Maruyama et al. [20]. Generally, C atoms and OH species are decomposed on the catalyst surface from alcohol molecules. In the case of this work, the infusion CVD is done at atmospheric pressure in which a relatively high concentration of carbon atoms is obtained and the catalyst size is much greater than a typical SWNT diameter, therefore, the MWNT growth is preferential in this sense. We believe that, the growth mechanism of MWNTs is probably governed by the hollow-cored growth [35]. Namely, after adsorption and decomposition of ethanol molecules at the Ni surface, diffusion of carbon atoms along the external surface is faster than the interior, hence, graphitic hollow-cored CNT is formed.

4. Conclusion

MWNTs have been successfully synthesized from ethanol vapor in the large-scale production system without a carrier gas by the infusion CVD method. The technique for the electrical resistivity measurement of the bulk MWNTs has been demonstrated. The exponentially correlation of the resistivity and the I_D/I_G ratio was observed, suggesting that the measuring method provides the simple tool to monitor the degree of structural defects of CNTs.

Acknowledgements

This work was supported by the Thailand Research Fund (TRF). The authors would like to thank Mr. Thirapol Chinda and Dr. Torranin Chairuangsri for their assistances with FE-SEM and TEM operations and Mr. Ekkapong Kuntaruk for his help in Raman spectroscopy measurement.

References

[1] S. Iijima, Nature 354 (1991) 56.
[2] P.J.F. Harris, Carbon Nanotubes and Related Structures: New Materials for the 21st Century, Cambridge University Press, Cambridge, 1999.
[3] K.T. Lau, D. Hui, Compos. B-Eng. 33 (2002) 263.
[4] G.G. Tibbetts, G.P. Meisner, C.H. Olk, Carbon 39 (2001) 2291.
[5] V.V. Simonyan, J.K. Johnson, J. Alloys Compd. 330–332 (2002) 659.
[6] X. Li, F. Kang, W. Shen, Carbon 44 (2006) 1298.
[7] E. Frackowiak, V. Khomenko, K. Jurewicz, K. Lota, F. Béguin, J. Power Sources 153 (2006) 413.
[8] C.J. Lee, J. Park, S. Han, J. Ihm, Chem. Phys. Lett. 337 (2001) 398.
[9] S. Honda, Y.G. Baek, K.Y. Lee, T. Ikuno, T. Kuzuoka, J.-T. Ryu, S. Ohkura, M. Katayama, K. Aoki, T. Hirao, K. Oura, Thin Solid Films 464 (2004) 290.
[10] D. Sarangi, I. Arfaoui, J.M. Bonard, Physica B 323 (2002) 165.
[11] H. Dai, J.H. Hafner, A.G. Rinzler, D.T. Colbert, R.E. Smalley, Nature 384 (1996) 147.
[12] B. Philip, J.K. Abraham, A. Chandrasekhar, V.K. Varadan, Smart Mater. Struct. 12 (2003) 935.
[13] O.K. Varghese, P.D. Kichambre, D. Gong, K.G. Ong, E.C. Dickey, C.A. Grimes, Sens. Actuators B: Chem. 81 (2001) 32.
[14] A.C. Dillon, A.H. Mahan, P.A. Parilla, J.L. Alleman, M.J. Heben, K.M. Jones, K.E.H. Gilbert, Nano Lett. 3 (2003) 1425.
[15] S. Thongtem, P. Singjai, T. Thongtem, S. Preyachoti, Mater. Sci. Eng. A 423 (2006) 209.
[16] G. Gulino, R. Vieira, J. Amadou, P. Nguyen, M.J. Ledoux, S. Galvagno, G. Centi, C. Pham-Huu, Appl. Catal. A 279 (2005) 89.
[17] Y. Li, X.B. Zhang, X.Y. Tao, J.M. Xu, W.Z. Huang, J.H. Luo, Z.Q. Luo, T. Li, F. Liu, Y. Bao, H.J. Geise, Carbon 43 (2005) 295.
[18] C. Singh, M.S.P. Shaffer, K.K.K. Koziol, I.A. Kinloch, A.H. Windle, Chem. Phys. Lett. 372 (2003) 860.
[19] H. Hou, A.K. Schaper, Z. Jun, F. Weller, A. Greiner, Chem. Mater. 15 (2003) 580.
[20] S. Maruyama, R. Kojima, Y. Miyauchi, S. Chiashi, M. Kohno, Chem. Phys. Lett. 360 (2002) 229.
[21] T. Okazaki, H. Shinohara, Chem. Phys. Lett. 376 (2003) 606.
[22] S. Chiashi, Y. Muramaki, Y. Miyauchi, S. Maruyama, Chem. Phys. Lett. 386 (2004) 89.
[23] A. Okamoto, H. Shinohara, Carbon 43 (2005) 431.
[24] D. Nishide, H. Kataura, S. Suzuki, S. Okubo, Y. Achiba, Chem. Phys. Lett. 392 (2004) 309.
[25] J. Liu, M. Shao, X. Chen, W. Yu, X. Liu, Y. Qian, J. Am. Chem. Soc. 125 (2003) 8088.
[26] W. Zhang, D. Ma, J. Liu, L. Kong, W. Yu, Y. Qian, Carbon 42 (2004) 2329.
[27] H. Dai, E.W. Wong, C.M. Lieber, Science 272 (1996) 52.
[28] T.W. Ebbesen, H.J. Lezec, H. Hiura, J.W. Bennett, H.F. Ghaemi, T. Thio, Nature 382 (1996) 54.
[29] R.Z. Ma, C.L. Xu, B.Q. Wei, J. Liang, D.H. Wu, D.J. Li, Mater. Res. Bull. 34 (1999) 741.
[30] A.G. Rinzler, J. Liu, H. Dai, P. Nikolaev, C.B. Huffman, F.J. Rodríguez-Macías, P.J. Boul, A.H. Lu, D. Heymann, D.T. Colbert, R.S. Lee, J.E. Fischer, A.M. Rao, P.C. Eklund, R.E. Smalley, Appl. Phys. A 67 (1998) 29.
[31] A.M. Valiente, P.N. López, I.R. Ramos, A.G. Ruiz, C. Li, Q. Xin, Carbon 38 (2000) 2003.
[32] Y.H. Li, J. Wei, X. Zhang, C. Xu, D. Wu, L. Lu, B. Wei, Chem. Phys. Lett. 365 (2002) 95.
[33] C. Qin, X. Shi, S.Q. Bai, L.D. Chen, L.J. Wang, Mater. Sci. Eng. A 420 (2006) 208.
[34] K. Hata, D.N. Futaba, K. Mizuno, T. Namai, M. Yumura, S. Iijima, Science 306 (2004) 1362.
[35] C. Pan, Y. Liu, F. Cao, J. Wang, Y. Ren, Micron 35 (2004) 461.